UNIVERSITY OF OKLAHOMA

GRADUATE COLLEGE

USE CAPACITANCE-RESISTANCE MODEL TO CHARACTERIZE WATER FLOODING IN A TIGHT OIL RESERVOIR

A THESIS

SUBMITTED TO THE GRADUATE FACULTY

in partial fulfillment of the requirements for the

Degree of

MASTER OF SCIENCE

By

KAILEI LIU
Norman, Oklahoma
2017

USE CAPACITANCE-RESISTANCE MODEL TO CHARACTERIZE WATER FLOODING IN A TIGHT OIL RESERVOIR

A THESIS APPROVED FOR THE
MEWBOURNE SCHOOL OF PETROLEUM AND GEOLOGICAL ENGINEERING

BY

_____
Dr. Xingru Wu, Chair

_____
Dr. Bor-Jier Shiau

_____
Dr. Zulfiquar Reza

Dedication

To my dear parents:

Dehua Liu

Zhimin Zhou

Acknowledgements

I would like to express my deepest gratitude and appreciation to my supervisor, Dr. Xingru Wu, for his guidance and financial support during my graduate studies at the University of Oklahoma. With his assistance, expertise and trust, I was able to finish this research in one and a half years. Dr. Xingru Wu offered me the opportunity to join the master's program and taught me how to conduct research in a scientific and professional way. I would also like to express my gratitude and appreciation to Dr. Bor-Jier Shiau and Dr. Zulfiquar Reza for serving as my committee members and reviewing my work.

I would also like to express my gratitude and appreciation to Dr. Wei Tian for his assistance and guidance during my graduate studies. I would also like to thank my officemates and colleagues, Jiabo He and Yifu Han, for their comments and advice on my research. I also appreciate my friends at the University of Oklahoma. I would also like to thank the friends that I met while I was an undergraduate student at the University of Oklahoma. In our spare time, we discussed our dreams for the future. With their companionship, my seven years at the University of Oklahoma was interesting and memorable.

Furthermore, I would like to thank the faculty and staff of the Mewbourne College of Earth and Energy and the Mewbourne School of Petroleum and Geological Engineering. As an overseas student, they often helped me during my seven years at the University of Oklahoma; I enjoy this country and those whom I have met.

Finally, I would like to thank my mother and father. Their love and unconditional support have encouraged me to successfully complete this work.

Table of Contents

List of Tables

List of Figures

Abstract

Gaither Draw Unit is a heterogeneous and tight formation with an average permeability of 0.1 mD. After more than 1.7 MMSTB water has been injected, there was no clear signal indicating the injected water from any producer. However, knowing the distribution of injected water is critical for future well planning and quantifying the efficiency of injection. The objective of this study is to show how the Capacitance-Resistance Model (CRM) was used to study this field and how the results were validated using traditional reservoir simulation.

The CRM model quantitatively describes the connectivity and the degree of fluid storage between injectors and producers only from injection and production rate data. On the basis of material balance, signals from injectors to producers can be represented in the CRM model. The connectivity between each injector/producer pair of a selected portion of the field is estimated by using a constrained nonlinear multivariable optimization technique.

The fitting results of the connectivity and the time constant through the CRM analysis indicate the regional permeability heterogeneity, which is consistent with Computer Modelling Group, Ltd. (CMG) full field modelling. The time constants conform to the low permeability of a tight formation. The history matched CMG full field model and results from the CRM analysis both present similar pressure distributions. It indicates that the majority of the injected water mainly saturates the regions surrounding the injectors, and the low transmissibility prevents pressure dissipation.

Chapter 1 Introduction

1.1 Problem Statement

In a water flooding project, water is injected through injection wells to supplement the energy of the reservoir and displace oil towards production wells to enhance oil production. The key factor of a water flooding project is sweep efficiency, which is affected by the reservoir heterogeneity. A successful water flooding project relies on the accurate description of the reservoir and prediction of the well performance; therefore, a suitable model that can history match past reservoir behavior is always important. In order to find the most efficient manner to produce oil, this model can be further used to predict production performance under different oil field development schemes, such as different well patterns and in-fill drilling. There are generally six approaches to evaluating and predicting reservoir performance (Cao, 2014). Figure 1-1 shows the complexity and effort required to conduct each evaluation approach. All approaches involve history matching.

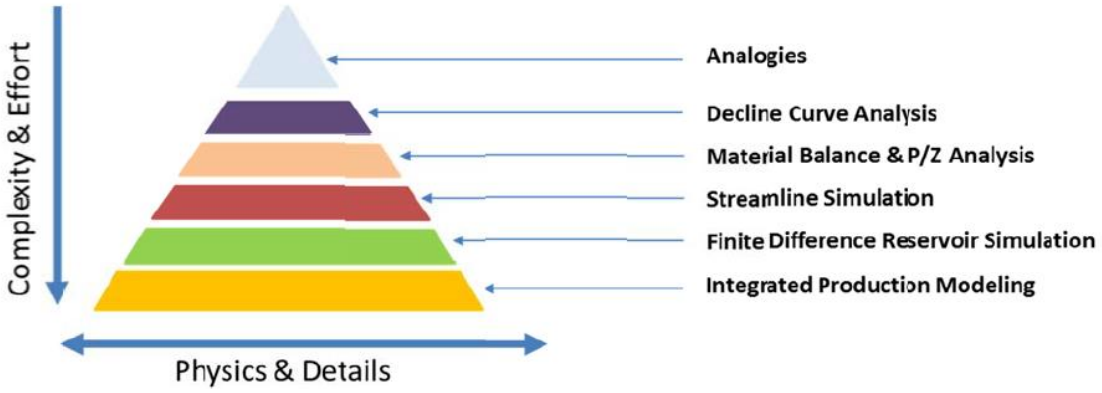

Figure 1-1 —Complexity and effort vs. physics and details of different approaches in reservoir evaluation (Cao, 2014).

However, due to the uncertainty of petrophysical/fluid properties, all approaches of history matching are inverse problems. For example, traditional reservoir simulators, which use the finite difference approach to solve partial differential equations can evaluate a reservoir by requiring many uncertain inputs, such as permeability, porosity, fluid properties, compressibility, saturation profile, and others. Consequently, the procedure of history matching in traditional reservoir simulation is often time consuming and computationally expensive. Furthermore, the difficulty of data acquisition in the field would result in a challenging history matching process. Even with an accepted fit between field observations and the results of numerical simulation, the matching model may not represent the actual condition of the reservoir due to the non-uniqueness of inverse problem solutions.

Compared with traditional reservoir simulators, Capacitance-Resistance Model requires only the injection rates of each injector and the production rates of each producer as input to evaluate reservoir performance. The connectivity and the time constant that are estimated by fitting production rates can provide useful information about geological features and reservoir heterogeneity. With a clear understanding of reservoir heterogeneity, flow barriers and high permeable zones can be identified. Significant reservoir heterogeneity can lead to poor sweep efficiency. These characteristic features make the CRM model a unique and practical tool to investigate water flooding projects.

1.2. Objectives of Research

The objectives of this study are as follows:

1. Applying the CRM model to a tight oil reservoir to study the interwell connectivity and understand the reservoir heterogeneity. The quantitative results can be obtained by using a nonlinear optimization technique; the CRM solver is coded and executed in MATLAB.
2. Several issues with applying the CRM model in the tight oil reservoir are addressed, and solutions to these issues are suggested.
3. Based on the CMG full field history matching result and the CRM model fitting results, a better understanding of the injected water distribution is achieved.
4. The predicted production rates of the CRM model and the CMG full field model are compared and discussed.

1.3. Thesis Outline

Chapter 2 presents a literature review of the technologies used to study water flooding and its response. First, traditional approaches of interwell connectivity and reservoir heterogeneities evaluation with their associated limitations and disadvantages are discussed. Traditional technologies in studying water flooding include tracer test, well test, and geochemistry. Second, the development of Capacitance Resistance Model is reviewed. The parameters of the CRM model and their associated physical meanings are discussed. Finally, this chapter discusses recent contributions to the CRM model.

Chapter 3 talks about the mathematical derivation of the CRM model. It starts with a macroscopic material balance equation, and then combines with linear productivity model to obtain a basic ordinary differential equation. Based on three different control

volume approaches, the semi-analytical solutions are reviewed and compared. The assumptions of the CRM model are addressed and the solver, which is used to determine the parameters in the CRM model, is discussed.

Chapter 4 discusses a field case study of conducting the CRM analysis in tight oil reservoir. This chapter starts with a brief introduction to the field case area by presenting geological and geophysical information, reservoir fluid properties, and drilling and completion information. Afterwards, several limitations of using the CRM model in this area are addressed. Then, procedures to overcome these limitations are suggested. Finally, the results of interwell connectivity and the time constant is shown and discussed. The CMG full field model is used to make a comparison between results.

Chapter 5 discusses the CRM model as a predictive tool. The predicted production rates to December 2019 by the CRM model and CMG full field model are discussed and compared.

Chapter 6 provides conclusions of this research and some future works are recommended.

Chapter 2 Literature Review

The purpose of water flooding is to maintain the reservoir pressure and displace oil to the producer. Knowing where the injected water went is critical in well placement, enhanced oil recovery, and production management. In reservoir engineering, there are a few tools, direct and indirect, that people use to achieve this objective. In this session, tracer test, well test, geochemistry and the CRM model will be discussed, and their associated advantages and disadvantages will be evaluated.

2.1 Tracer Test

Tracer test can be used to infer interwell connectivity and understand reservoir heterogeneities (Du & Guan, 2005). By adding different tracers with the injected water at different injection wells and monitoring tracers in the production fluid at surrounding producing wells, the flow behavior can be identified.

Chemical tracers and radioactive tracers are commonly used in oil fields. For the aspect of chemical tracers, water soluble inorganic salts, fluorescent dyes, and specific alcohols are widely employed. Since both the soluble inorganic salts and the formation are negatively charged, this kind of tracer is not easily absorbed by the formation. As a result, this kind of tracer is more easily captured at a production well. Fluorescent dyes, another kind of water-soluble tracer, are easily absorbed into the formation. They could be applied into testing the fracture connectivity because of the short remaining time in the fracture caused by its high permeability. The oil soluble tracer usually has limited applications because of its low bio-stability.

The radioactive tracer mainly refers to the isotope tracer, especially neon compounds. The advantage of this kind of tracer is that it can directly obtain reservoir information from radioactivity rather than by capturing and evaluating fluid samples. However, radioactive tracers have limited application because of their radioactivity and excessive cost. As radioactive tracer develops, stable radioactive tracers become more widely used in field applications.

Qualitative results from the arrival and non-arrival of the specific tracer at producing wells can show the connection between the injector and targeted producers. For instance, if a designed tracer is injected from a particular injection well and it is produced at a particular surrounding production well, then the two wells are hydraulically connected; otherwise, these two wells may be not connected. Furthermore, the breakthrough timing at different producers may indicate the connectivity between the pairs of wells. Quantitative results can be determined by comparing the different fractions of tracer response at surrounding production wells. The numerical method can be used to interpret tracer test results. The objective of this method is to history match interwell tracer data by changing the appropriate reservoir parameters. These reservoir parameters can also be used to infer reservoir heterogeneities.

Compared to the numerical simulation method, the reservoir characteristics, like residual oil saturation, could be identified by tracers using the method of moments (MoM). As one of the advantages of the MoM, there is not much information required to interpret the tracer results (Cockin et al., 2000). Within the application of tracers, the MoM could be used with both the single well chemical tracer test (SWCTT) and partitioning interwell tracer test (PITT). Nevertheless, for both SWCTT and PITT, the

key assumption is that only one phase should be mobile. In order to relax this assumption, an improved MoM was introduced to analytically estimate the mobile phase saturations through SWCTT. On the other hand, unlike the pure water injection in unimproved SWCTT, the mixture of water and oil could be injected (Tian, 2017). Sinha et al. (2004) estimated oil saturation by using the MoM in PITT, and also relaxed this assumption.

Wagner (1977) reported tracer tests in four field case studies to diagnose the interwell reservoir heterogeneity. In the Levelland Unit Tertiary miscible pilot, by comparing the predicted and actual arrival time of the peak tracer concentrations, the simulation model could give a confidence to provide guidelines for attaining safe radiation limits in other tracing programs. In the second field case in the Little Buffalo Basin in Wyoming, the operator used tracers to identify poor communication of the particular well and the loss of the injected fluids outside of the pattern area. As a result, the production rate was augmented after the high-volume acid stimulation. Another area of the Little Buffalo Basin in Wyoming was discussed as the third area. Through the tracer test and injection of the tritiated water, ethyl alcohol and isopropyl alcohol as tracers, the problem of that area was identified as production discontinuity. The last area is the South Swan Hill Unit hydrocarbon, miscible flood in Alberta, Canada. After tracer test, several areas have shown low sweep efficiency due to the early breakthrough of solvent and water tracer.

Furthermore, the radioactive tracer also has been used to diagnose the interwell heterogeneity. Specifically, field case shows that carbon-14, cobalt-57, cobalt-60 and tritium could be used in any pattern waterflood to investigate the injected fluid movement in a multipay, discontinuous reservoir (Dhooge et al., 1981).

The disadvantage of tracer tests is that it may last long to observe the tracer response at producing wells. Furthermore, the problem of poor sampling defeats the purpose of tracer test. The worst case is that the tracer cannot be found in any observation wells, which could be caused by the unknown high permeable zone or leakage from the wellbore completions.

2.2 Well Test

There are many well test methods, such as build up test, draw down test, pulsing pressure test, and interference test. Their fundamental idea is to analysis the pressure changing to obtain perspective of the reservoir characteristic. Interference and pulse well tests can be used to infer well communications and reservoir heterogeneities (Kamal, 1983). In interference well tests, there are one active well and one or more surrounding observation wells. The bottom hole pressure of observation wells is recorded when the production rates of active well are changed. By analyzing the bottom hole pressure profile of observation wells, whether two or more wells are in pressure communication can be determined. When two wells are connected, the average permeability and average storage capacity can be quantitatively obtained.

The pulse well test is a modified version of interference well test with shorter and smaller pressure changes. Compared to conventional interference well test, the signal by the stimulus of active well can be identified more effectively. If the interwell connectivity needs to be determined, multiple well tests could be recommended.

Vela and Mckinley (1970) investigated how areal heterogeneity affects pulse test result between a well pair. They gave an equation to calculate the influence radius of the

pulse well. Through using this equation, the rectangle influenced by two wells could be determined. Woods (1970) gave a mathematical model to determine the pressure from two-zone reservoir through combination of two single well. Furthermore, the characteristics of the reservoir could be obtained. However, this prediction would be accurate only if wellbore was undamaged or uniformly damaged.

Araujo et al. (1988) gave an example of interference and pulse tests analysis in a heterogeneous naturally fracture reservoir. They concluded that the effective permeability and shape factor would be close to the arithmetic average values in the heterogeneous naturally fracture reservoir. Furthermore, the permeability anisotropy values could also be obtained from the pulse test through the method they provided. However, this specific study was based on the single well test.

One of the major disadvantage of pressure changing well test is the long shut in time required, which causes a big economic loss. On the other hand, production rate also could be monitored and analyzed to obtain the reservoir characteristic. The operator does not have to shut in the well. The obviously disadvantage is that the pressure changing may be too small to observe.

2.3 Geochemistry

The application of chromatographic fingerprinting can help to infer reservoir continuity (Slentz, 1981). By doing chromatographic analysis towards production fluid at different producers, a fingerprint of each fluid sample can be identified. With the information of fingerprints, reservoir continuity can be inspected. Therefore, the reservoir geochemistry technique is employed in the reservoir appraisal as an alternative method

of the conventional way. The key idea of the investigation of the reservoir continuity by the geochemistry is that the reservoir fluids are often compositionally heterogeneous (Larter & Aplin, 1994). Furthermore, through the study of reservoir geochemistry, a better understand of rock/fluid interactions can be obtained.

Kaufman et al. (1997) used the geochemistry analysis and oil fingerprinting to characterize the Greater Burgan Field. There were many works done in their study. One of the work they done is to study the reservoir continuity. Identifying the sample oil fingerprints and incorporating the results into a numerical simulation, they conclude that the oil could come from different units of reservoir and the near wellbore damage can be identified. However, reservoir heterogeneity cannot be described quantitatively by this technique.

One advantage of reservoir geochemistry analysis is the cost-effective compared with other methods, such as the stable radioactive tracer. Another advantage is that there is no effect from the well intervention or loss production. A third advantage is that the communication behind casing could exists. Under this condition, the information could be still valid (Nicolle et al., 1997).

The disadvantage of this method is that the connectivity between wells can be only determined qualitatively rather than quantitatively. Therefore, the geochemistry method has to be used with other techniques.

2.4 Capacitance-Resistance Model

In the CRM model, the reservoir medium is regarded as a resistor-capacitor circuit that converts electronic potential (input signal) to voltage (output signal), where the input

signal is injection rates and the output signal is production rates (Cao, 2014). In this thesis, the injection rate is injected water rates and the production rate means the total liquid production rates. There are two types of unknown parameters, interwell connectivity and the time constant between each injector/producer pair, which can be obtained by applying nonlinear optimization to solve the CRM model using injection/production rates as input.

Albertoni and Lake (2003) used a multivariate linear regression approach to determine the connectivity between each injector/producer pair by only analyzing the injection and production data. In this approach, the production rates of a specific producer are regarded as the sum of a portion of injection rates of surrounding connected injection wells (multiple producers case). Based on the balance condition of field injection rates and production rates, three different approaches are introduced to quantitatively infer connectivity (Albertoni, 2003). In the presence of dissipation effect, the diffusivity constants are introduced to each injector/producer pair to transform the injection rates to effective injection rates, which are the actual signals that the producer will receive.

Gentil (2005) investigated the physical meaning of the weights between each injector/producer pair. He used a parallel flow analogy to conclude that the weights can also be calculated by using following equation:

$$\beta_{ji} = \frac{T_{ji}}{\sum_J T_{ji}} \tag{2.1}$$

Here, the physical meaning of the weights is the ratio of the transmissibility between an injector and a producer to the sum of the transmissibility between the same injector and all connected producers. Based on this physical meaning, the weights can also be regarded as allocation factors that determine how much injected water from one injector goes to each connected producer. This makes the weights always positive numbers. In addition,

in an idealistic condition, the sum of the weights associated with one injector should be equal to one. The larger the weight for an injector/producer pair is, the more influence the injector has on the producer. This provides a quantitative way to describe interwell connectivity.

Instead of using diffusivity filter to capture the dissipation effect in the reservoir medium, Yousef (2006) introduced a nonlinear signal processing model to represent how reservoir medium transfers injection rates to effective injection rates. In this nonlinear signal processing model, the bottom hole pressure data can be incorporated with the injection and production rate data to infer interwell connectivity. Since this model combines two well-known equations with straightforward physical meaning, it becomes more reliable and efficient than diffusivity filters. The discrete form of most fundamental equation in the CRM model is (Yousef, 2005):

$$\hat{q}_j(n) = \beta_p q_j(n_0) e^{\frac{-(n-n_0)}{\tau_P}} + \sum_{i=1}^{i=I} \beta_{ij} i'_{ij}(n) + \sum_{k=1}^{k=K} v_{kj}[p_{wf_{kj}} e^{\frac{-(n-n_0)}{\tau_{kj}}} - p_{wf_{kj}}(n) + p'_{wf_{kj}}(n)] \tag{2.2}$$

Where,

$$\mathrm{i}'_{ij}(n) = \sum_{m=n_0}^{m=n} \frac{\Delta n}{\tau_{ij}} e^{\frac{(m-n)}{\tau_{ij}}} i_{ij}(m) \tag{2.3}$$

$$P'_{wf_J}(n) = \sum_{m=n_0}^{m=n} \frac{\Delta n}{\tau_J} e^{\frac{(m-n)}{\tau_j}} P_{wf_j}(m) \tag{2.4}$$

In Eq. 2.2, there are six types of unknown parameters (β_p, τ_p, β_{ij}, τ_{ij}, v_{kj} and τ_{kj}) in the model. β_p and τ_p are empirical parameters of mathematical approximation and simplification of primary production effect. β_{ij} is interwell connectivity between each injector/producer pair. τ_{ij} is the time constant between each injector/producer pair. v_{kj} is the coefficient of bottom hole pressure term in the CRM model. τ_{kj} is the time constant associated with bottom hole pressure term. β_{ij} and τ_{ij} describe the effect of injection rates on production rates. v_{kj} and τ_{kj} describe how changing bottom hole pressures of different producers affects production rates. When the bottom hole pressures of each producer are constant during analyzing period, v_{kj} of each producer becomes zero. It represents that production rates then are only related with primary production and injection rates. The physical meaning of β_{ij} is exactly the same as the weights in previous statistical approach. Consequently, it can also be used to quantitatively describe interwell connectivity. τ_{ij} determines how exactly the production rates are affected by injection rates, same as previous diffusivity filters. In other words, this type of coefficient is used to calculated effective injection rates in this model.

2.5 Recent Developments in the CRM Model

Sayarpour (2009) derived three continuity equations of the CRM model based on three different control volume approaches and gave semi-analytical solutions. For each control volume approach, the number of unknown parameters depends on the number of injectors and producers. The reservoir can be imaged as a tank that only has one pseudo-injector and one pseudo-producer, where the pseudo-injector or pseudo-producer is

combined from all the real injectors or producers. In this case, the rates of the pseudo-well should be equal to the sum of rates from all real wells. This control volume approach, denoted as Capacitance-Resistance Model Tank (CRMT) only evaluates the whole reservoir (Figure 2-1). Reservoir properties and interwell connectivity can be determined by two unknown parameters.

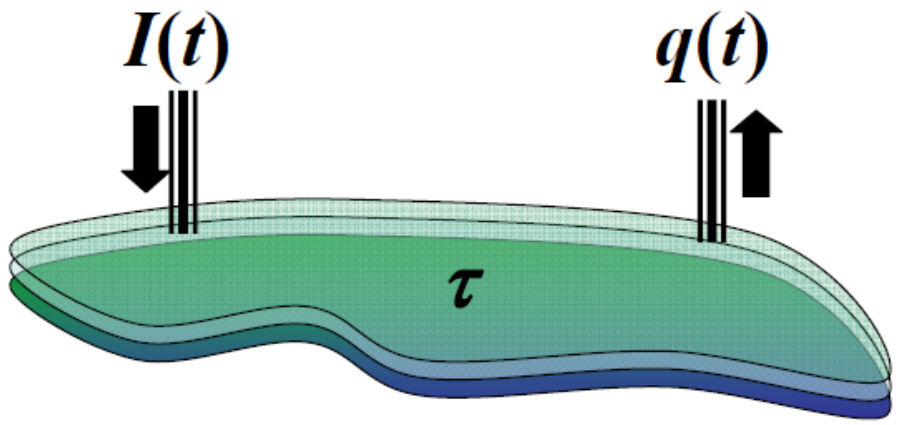

Figure 2-1 —Investigation area of the CRMT: drainage volume by pseudo-injection well and pseudo-production well (Sayarpour, 2009).

When the control volume is considered as the drainage volume around a producer, the Capacitance-Resistance Model Producer (CRMP) should be used. The time constant for producer *j* is based on the drainage volume around producer *j* (Figure 2-2). The physical meaning of interwell connectivity is the same as previous weights in statistical approach. Moreover, the number of unknown parameters is $N_{pro} \cdot (N_{inj}+2)$. From those parameters, the properties of drain volume around each producer can be investigated.

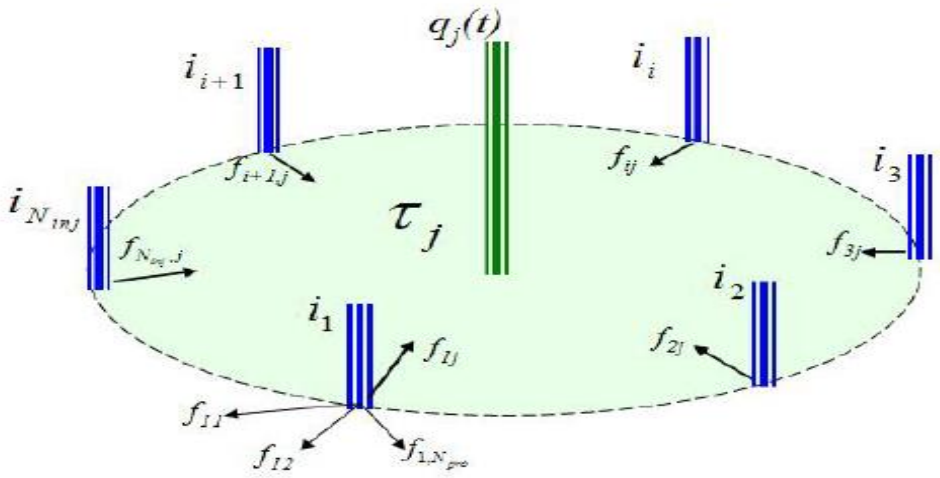

Figure 2-2 —Investigation area of the time constant in the CRMP: drainage volume around each producer (Sayarpour, 2009).

The last control volume approach, denoted as Capacitance-Resistance Model Injector Producer (CRMIP), is based on the same ordinary differential equation as the CRM model. As shown in Figure 2-3, the investigation of area is interwell region between each injector/producer pair, which is different from previous CRMT and CRMP approaches. The number of unknown parameters is $N_{pro} \cdot N_{inj} \cdot 3$.

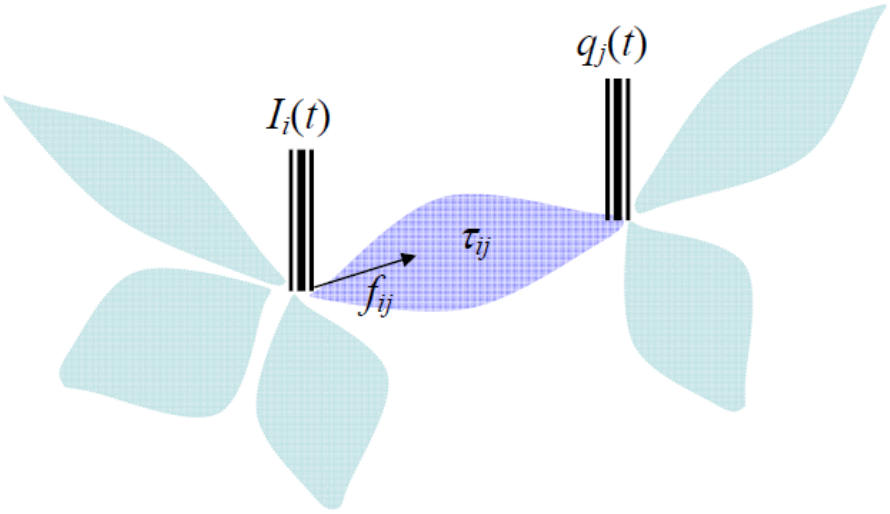

Figure 2-3 —Investigation area of the time constant in the CRMIP: drainage volume for each injector/producer pair (Sayarpour, 2009).

Since determination of unknown parameters requires a multivariate nonlinear regression process, more unknown parameters mean there are more data points required necessarily to obtain accurate result (Yousef, 2005). The number of data points refers to injection/production rates time periods. For instance, if injection/production rates of 100 months are available, the number of data points is 100. By using three different control volume approaches, reservoir properties at various scales can be investigated, depending on the amount of data points available.

In the field case, the data of bottom hole pressure are often documented infrequently or are unavailable. However, the interwell connectivity can be inferred more accurately by the CRM model with both flow rates and bottom hole pressure known. To extend the application of the CRM model in the field case, Kaviani (2012) provided a modified version of the CRM model: segmented CRM. There is a new term, $\beta'_{0j}(s)$,

added into the CRM model to account for the shift in production rates caused by changes in the bottom hole pressure.

One major assumption of the CRM model is that the parameters do not change during the analyzing period. That means in selected period and area, the number of production wells must remain constant in order to successfully apply the CRM model. However, there are always new producers added in the field case. Once a new producer is added into the field, the whole system changes, and the weights between each injector/producer pair need to be updated with a new analysis period. To overcome this shortage, Soroush et al. (2013) introduced the compensated CRM. The relationship between production rates before and after changes in the number of producers is established. The compensated CRM successfully handle the problem of shutting or adding producers. This method significantly lowers the number of unknown parameters in the CRM model.

Chapter 3 Methodology

In this chapter, the mathematical derivation of the CRM model is discussed in detail. The mathematical derivation starts with a governing material balance equation. Then, the governing material balance equation is combined with a linear productivity model to obtain an ordinary differential equation. The semi-analytical solution of the ordinary differential equation forms the CRM model. Assumptions are discussed after the mathematical derivation. Finally, the solver used to solve the CRM model is introduced.

3.1 Mathematical Derivation

For a case with one injector and one producer, the idea of the material balance equation is that the mass difference of phase I in an arbitrary control volume (CV) after a period of time, Δt, is equal to the mass difference between injected and produced fluid passing through this CV during Δt. By assuming an average constant density for phase I in CV, the mathematical expression becomes (Sayarpour, 2009):

$$\frac{d}{dt}\left(\bar{S}_i\bar{\rho}_j\bar{V}_p\right) = \rho_{i,in}q_{i,in} - \rho_{i,out}q_{i,out} \tag{3.1}$$

By applying the chain rule and rearranging the equation (Sayarpour, 2009):

$$\frac{1}{\bar{S}_i}\frac{d\bar{S}_i}{dt} + \frac{1}{\bar{\rho}_i}\frac{d\bar{\rho}_i}{d\bar{p}_i}\frac{d\bar{p}_i}{dt} + \frac{1}{\bar{V}_p}\frac{d\bar{V}_p}{d\bar{p}_i}\frac{d\bar{p}_i}{dt} = \frac{(\rho_{i,in}q_{i,in} - \rho_{i,out}q_{i,out})}{\bar{S}_i\bar{\rho}_j\bar{V}_p} \tag{3.2}$$

According to the definition of total compressibility, the following equations can be obtained by assuming that only two immiscible phases (water and oil) exist in the system (Sayarpour, 2009):

$$\frac{1}{\bar{S}_w}\frac{d\bar{S}_w}{dt} + (c_w + c_f)\frac{d\bar{p}_w}{dt} = \frac{(\rho_{w,in}q_{w,in} - \rho_{w,out}q_{w,out})}{\bar{S}_w\bar{\rho}_w\bar{V}_w} \tag{3.3}$$

$$\frac{1}{\bar{S}_o}\frac{d\bar{S}_o}{dt} + (c_o + c_f)\frac{d\bar{p}_o}{dt} = \frac{(0 - \rho_{o,out}q_{o,out})}{\bar{S}_o\bar{\rho}_o\bar{V}_o} \tag{3.4}$$

Since only water is injected in a water flooding project, the oil inflow on the right side of Eq. 3.4 becomes 0. Another assumption is that the density for all fluids in this system is constant and the capillary pressure effect is neglected. The following equation can be obtained by summing Eq. 3.3 and Eq. 3.4 and simplifying (Yousef, 2006):

$$c_t V_p \frac{d\bar{p}}{dt} = i(t) - q(t) \tag{3.5}$$

From this equation, one can conclude that the changes in the average reservoir pressure are due to the imbalance of field injection rates and production rates. This equation is also the governing material balance equation for the Capacitance-Resistance Model Tank, where $i(t)$ is the injection rates for the pseudo-injection well and $q(t)$ is the production rates for the pseudo-production well. The production rates can also be calculated by the following linear productivity model (Walsh & Lake, 2003):

$$q = J(\bar{p} - p_{wf}) \tag{3.6}$$

Substituting Eq. 3.6 into Eq. 3.5 to eliminate the average reservoir pressure:

$$\tau\frac{dq}{dt} + q(t) = i(t) - \tau J\frac{dp_{wf}}{dt} \tag{3.7}$$

Where,

$$\tau = \frac{c_t V_p}{J} \quad \text{(time constant)} \tag{3.8}$$

The solution of Eq. 3.6 is given by Yousef (2006):

$$q(t) = q(t_0)e^{-\frac{t-t_0}{\tau}} + \frac{e^{-\frac{t}{\tau}}}{\tau}\int_{\xi=t_o}^{\xi=t} e^{\frac{\xi}{\tau}} i(\xi)d\xi$$
$$+J\left[p_{wf}(t_0)e^{-\frac{t-t_0}{\tau}} - p_{wf}(t) + \frac{e^{-\frac{t}{\tau}}}{\tau}\int_{\xi=t_0}^{\xi=t} e^{\frac{\xi}{\tau}} p_{wf}(\xi)d\xi\right] \quad (3.9)$$

From Eqn.3.9, the production rates consist of the effect of primary production, injection input signal, and changing bottom hole pressure of the producer. By using superposition in time, Sayarpour (2009) gave a semi-analytical solution to Eq. 3.7:

$$q(t_n) = q(t_0)e^{-\left(\frac{t_n-t_0}{\tau}\right)}$$
$$+\sum_{k=1}^{n}\left\{\left(1-e^{\frac{-\Delta t_k}{\tau}}\right)\left[I^{(k)} - J\tau\frac{\Delta p_{wf}^{(k)}}{\Delta t_k}\right]e^{-\left(\frac{t_n-t_k}{\tau}\right)}\right\} \quad (3.10)$$

In multiple injector/producer case, the concept of the weights, as described in previous statistical approach in section 2.4, should be introduced due to multiple producers are often supported by one injector in the field case. Considering the control volume as the drainage volume around each producer, the ordinary differential equation for the CRMP becomes (Liang, 2007):

$$\tau_j\frac{dq_j}{dt} + q_j(t) = \sum_{i=1}^{N}\beta_{ij}i(t) - \tau_j J_j\frac{dp_{j_{wf}}}{dt} \quad (3.11)$$

Where,

$$\tau = \frac{c_t V_p}{J} \quad \text{(time constant)} \quad (3.12)$$

The semi-analytical solution to Eq. 3.11 is given by Sayarpour (2009):

$$q_j(t_n) = q_j(t_0)e^{-(\frac{t_n - t_0}{\tau_j})} + \sum_{k=1}^{n}\left\{\left(1 - e^{\frac{-\Delta t_k}{\tau_j}}\right)\left[\sum_{i=1}^{N}\beta_{ij}I_i^{(k)} - J_J\tau_j\frac{\Delta p_{j_{wf}}^{(k)}}{\Delta t_k}\right]e^{-(\frac{t_n - t_k}{\tau_j})}\right\} \quad (3.13)$$

Considering the control volume as interwell region between one injector and one producer, the ordinary differential equation for the CRMIP becomes (Yousef, 2006):

$$\sum_{i=1}^{I}\tau_{ij}\frac{dq_{ij}}{dt} + \sum_{i}^{I}q_{ij}(t) = \sum_{i=1}^{I}\beta_{ij}i_i(t) - \frac{dp_{wf_j}}{dt}\sum_{i=1}^{I}\tau_{ij}J_{ij} \quad (3.14)$$

Where,

$$\tau_{ij} = \frac{C_{t_{ij}}V_{p_{ij}}}{J_{ij}} \quad (3.15)$$

The semi-analytical solution to Eq. 3.14 is given by Sayarpour (2009):

$$q_j(t_n) = \sum_{i=1}^{N}q_{ij}(t_0)e^{-\left(\frac{t_n - t_0}{\tau_{ij}}\right)} + \sum_{k=1}^{n}\left\{\left(1 - e^{\frac{-\Delta t_k}{\tau_{ij}}}\right)\left[\beta_{ij}I_i^{(k)} - J_{iJ}\tau_{ij}\frac{\Delta p_{wf}^{(k)}}{\Delta t_k}\right]e^{-(\frac{t_n - t_k}{\tau_{ij}})}\right\} \quad (3.16)$$

Since the producers and injectors are considered as pseudo-wells in the CRMT, the parameters in the CRMT cannot provide useful information about interwell connectivity. The difference between the Capacitance-Resistance Producer and the Capacitance-Resistance Injector Producer is the number of the time constant, τ. In the CRMP, there is a time constant for each producer. In the CRMIP, there is a time constant for each injector/producer pair. However, the time constant controls the nonlinear part in the CRM equation. If the time constants are known, the CRM model becomes a linear

problem with only the weights unknown and can easily solved by a multiple linear regression (MLR).

In the field case, there are often lots of injectors and producers, which can generate large nonlinear optimization problem in the CRM model. In order to reduce the number of time constant and increase computation speed, the CRMP should always be used. When the bottom hole pressure is constant, there are only two types of parameters that require estimation in the CRMP. One is the weights that quantitatively describe interwell connectivity between each injector/producer pair. The other one is the time constants that quantitatively describe the storage effect of the reservoir medium around each producer. Figure 3-1 shows storage effect for different values of the time constant. As the time constant increases, more injected water is stored in the reservoir medium.

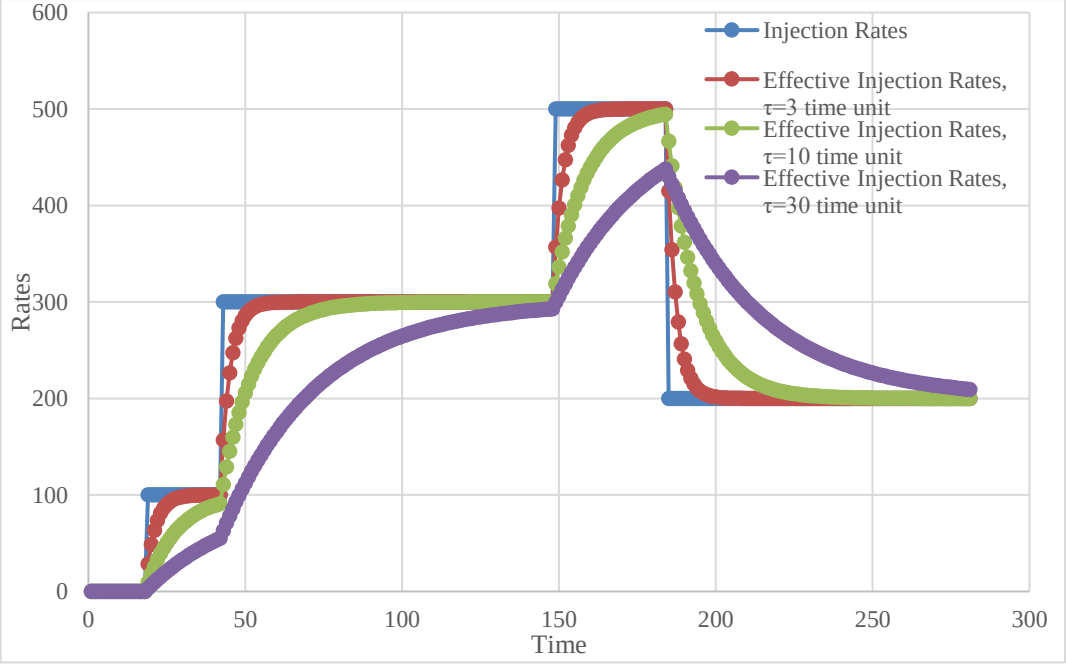

Figure 3-1 —Injection rates and associated effective injection rates at different values of the time constant.

3.2 Assumptions of the CRM Model

The major assumption of the CMR model is that all the parameters, including the weights and time constant, are constant during analyzing period. For the time constant, it mainly depends on total compressibility and productivity index. Therefore, this assumption is valid where there is no free gas and the reservoir fluids have a small compressibility. The productivity index will remain constant when there is no well re-completion and no major changes in well properties. For interwell connectivity, it depends on the transmissibility between each injector/producer pair. Consequently, the interwell connectivity will remain constant when no new producers are added during the analysis period.

3.3 The Solver of the CRMP

All unknown parameters in the CRM model or its modified version are determined by a nonlinear optimization process. The objective function is the mean square error (MSE) between actual total production rates and the estimated total production rates.

$$MSE = \sum_{j=1}^{K} [\hat{q}_j - q_j] \tag{3.17}$$

The nonlinear optimization process is to find sets of parameters that minimize the objective function. All parameters are determined by coding in MATLAB. The nonlinear optimization solver used to solve the CRM model is FMINCON in MATLAB, and the interior point algorithm is adopted to solve the problem. The MATLAB code is attached in Appendix B. Figure 3-2 illustrates the procedure to determine parameters.

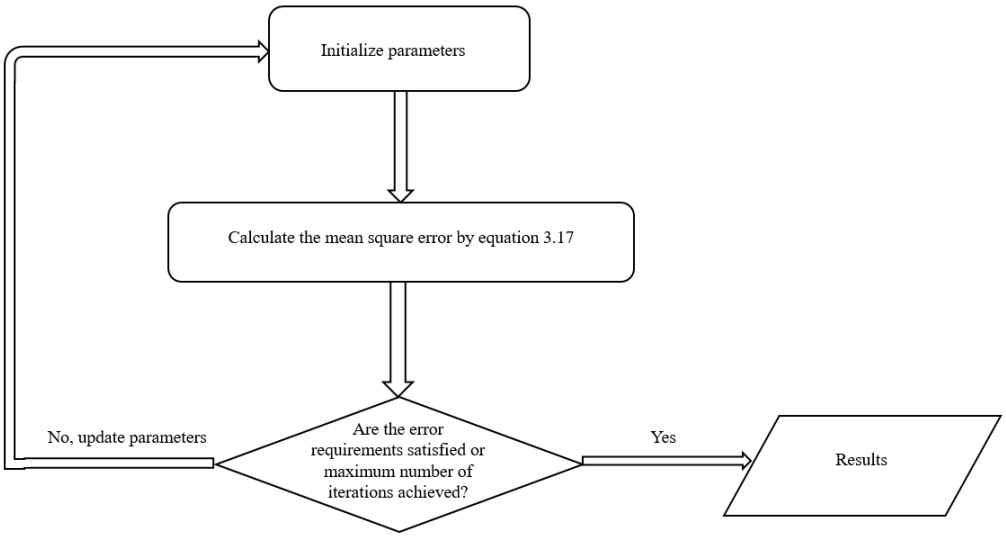

Figure 3-2 —Flow chart for parameter determination in the CRM model.

Chapter 4 Applying CRM in Field Case Study

4.1 Field Description

The study area, 21 Mile Butte and Gaither Draw Unit, is located in Parkman reservoir which is a part of the Powder River Basin. The Powder River Basin is located in southeast Montana and northeast Wyoming. Figure 4-1 shows the location of the Powder River Basin.

The Parkman Sandstone Member of the Upper Cretaceous Mesaverde Formation is the oldest sandstone member in a widespread cycle of Late Cretaceous regression. The Parkman reservoir consists of multiple stacked sands 5000 feet to 9500 feet deep. Figure 4-2 shows the stratigraphic column of the Upper Cretaceous strata in the Powder River Basin. There are three dominant lithologies of the Parkman reservoir. The first one is the prodelta shale and siltstone which includes very fine and well sorted sandstone. The second one is the medium-grained sandstone which lies on nearshore as coarsening-upward successions, and those sandstones were mixed up with siltstone. The last one is silt and mudstone which is gradual changing from carbonaceous to lignitic characteristics (Anna, 2009).

In summary, the Parkman reservoir consists of clean sands, cemented sands, and clays. Specifically, compositions of the Parkman sand are 49% quartz, 4% chert, 6% detrital dolomite, 11% feldspars, 22% micaceous schist, 1% micas, 5% altered volcanics and 2% other materials (Wilson, 1982).

Figure 4-3 shows the cross section of Powder River Basin. According to the sample core analysis and the log interpretation, the net pay of the Parkman reservoir is 60 feet with 10% average effective porosity. In addition, the Parkman reservoir is very

heterogeneous, that its porosity ranges from 2 to 12% and its permeability ranges from 0.0001 to 1md (Ingle et al., 2017). Figure 4-4 shows typical log curves of the Parkman reservoir.

The average pore pressure gradient of the Parkman formation is 0.37 psi/ft. The bubble point of the reservoir is less than 1000 psi and the reservoir is highly undersaturated. The fluid compressibility is $7*10^{-6}$ psi^{-1}, and the formation volume factor is 1.15 bbl/stb (Ingle et al., 2017). The fluid properties are calculated using Vasquez and Beggs correlation based on Gaither Draw Unit PVT reports. Table 4.1 shows fluid properties calculated at an undersaturated condition.

A total of 176 horizontal wells have been completed in the Parkman reservoir since 2009 (Ruhle & Orth, 2015). Multi-stage horizontal wells were drilled along north-south orientation. The well spacing is 160 acres, with 4 wells per section. Typical well designs for this area feature 25 fracturing stages along the long laterals, or 10 fracturing stages are placed along the short laterals. There are 280,000 lbs of proppant employed per stage for the standard well design. The total proppant consumption is 2.8 million lbs for the short lateral and 7.0 million lbs for the long lateral. Either the short lateral or the long lateral, the proppant concentration is 6 ppg (Ingle et al., 2017).

Table 4.1 — Fluid properties calculated at an undersaturated condition.

Pressure, psia	Solution gas, SCF/STB	Bo, rb/STB	Bg, rb/MSCF	Oil viscosity, cp	Gas Viscosity, cp
14.7	1.3	1.05	0.211744	2.792	0.0119
100	12.5	1.055	0.030767	2.581	0.012
500	84.1	1.089	0.005829	1.781	0.0126
1000	191.5	1.14	0.002735	1.263	0.0139
1500	309.9	1.196	0.001731	0.983	0.0156
2000	436.1	1.256	0.001259	0.81	0.0179
3000	705.7	1.383	0.000851	0.607	0.0234
4000	992.9	1.519	0.000691	0.492	0.0287
5000	1294	1.662	0.00061	0.417	0.0334
6000	1606.7	1.81	0.00056	0.364	0.0375
7000	1929.3	1.962	0.000527	0.325	0.0412

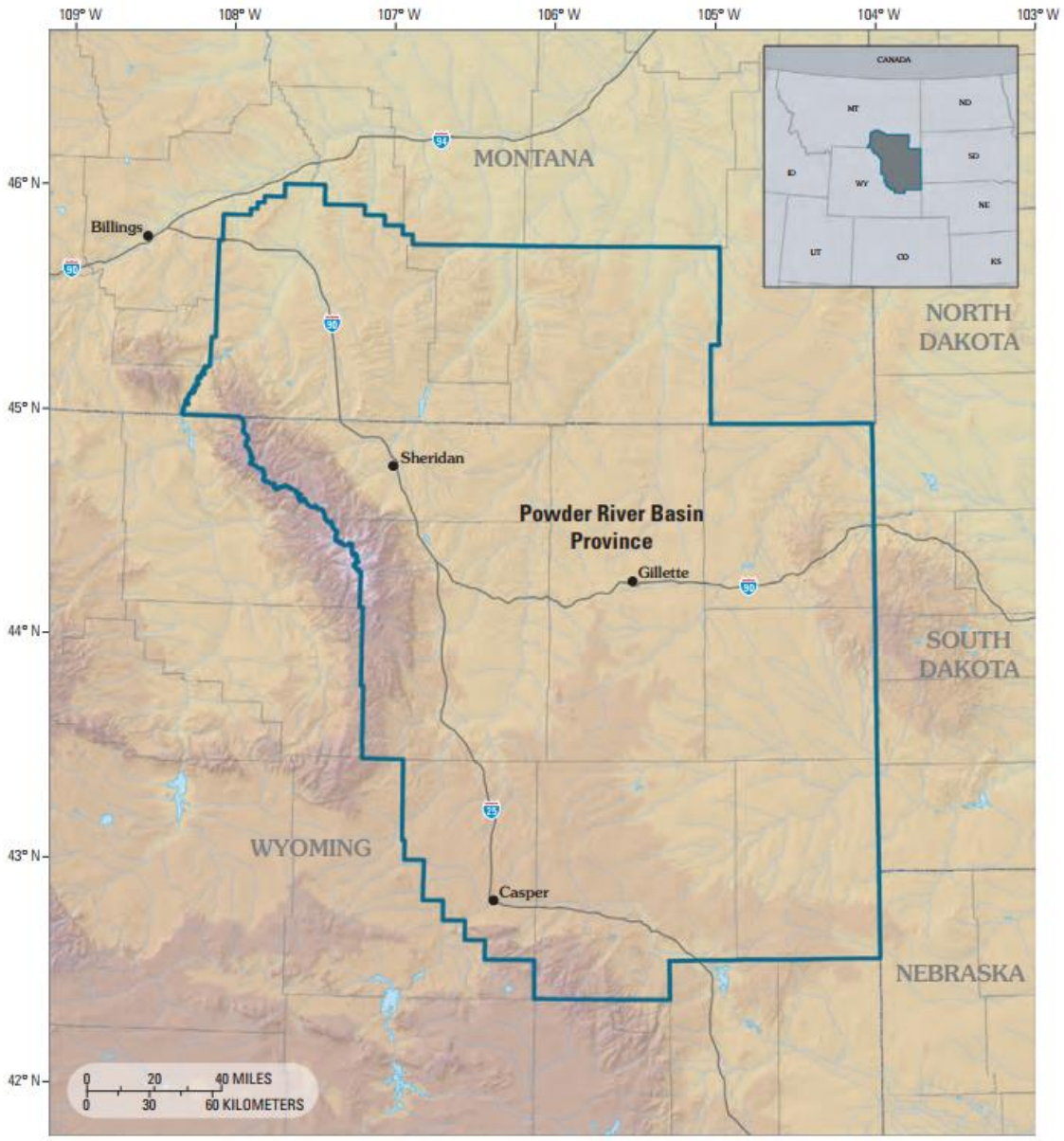

Figure 4-1 —Location of the Powder River Basin, southeast Montana and northeast Wyoming; blue line shows the boundary of the Powder River Basin (Anna, 2009).

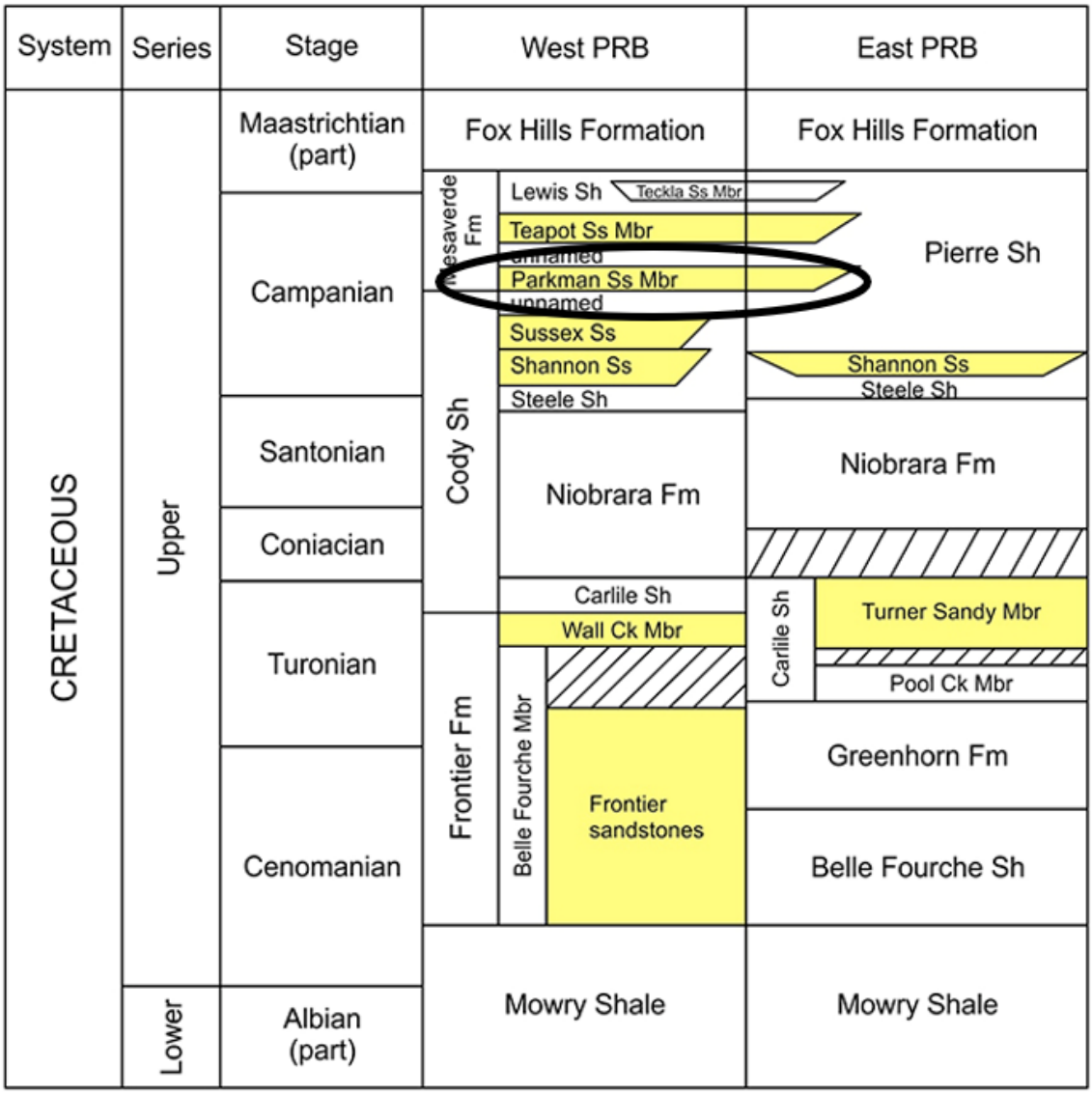

Figure 4-2 —Stratigraphic column of Upper Cretaceous strata in the Powder River Basin . Parkman source rock is circled. Mbr, member; Ck, Creek; Fm, formation; Sh, Shale; Ss, sandtone (Anna, 2009).

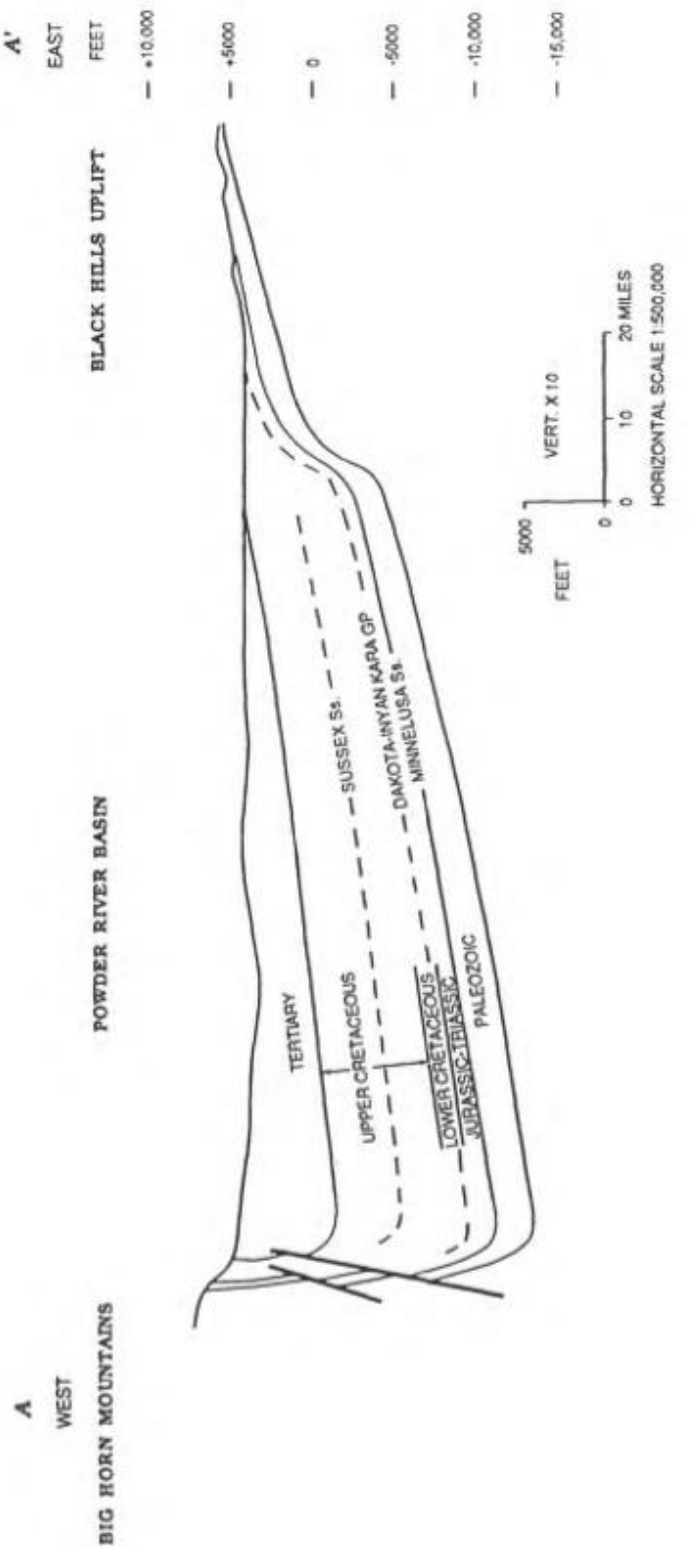

Figure 4-3 —Cross section of the Powder River Basin (Dolton et al., 1990).

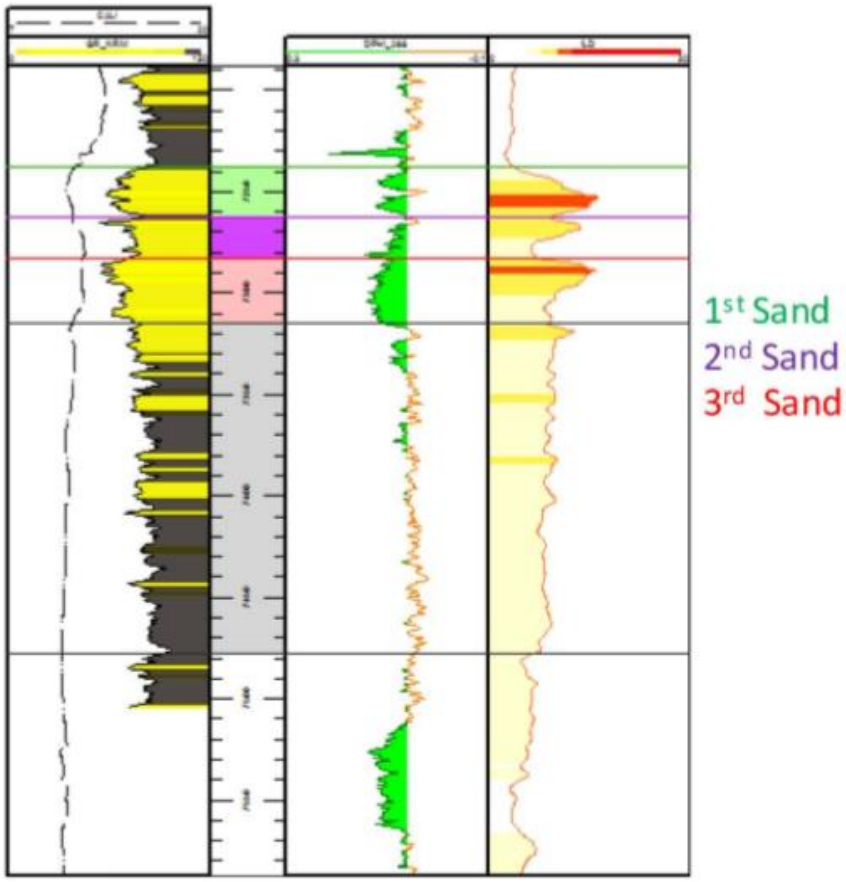

Figure 4-4 —Typical log curves of the Parkman reservoir (Ingle et al., 2017).

4.2 Review of Injection and Production Data

The field study area consists of two units: 21 Mile Butte and Gaither Draw Unit. There are seven injection wells in this field. Six of them are original production wells, and were converted to injection wells later. The first injection well began operating on 9/1/2010. The injection rates for all injectors are shown in Figure 4-5. For all injection wells, the injection rates were initially high, and then decrease dramatically due to the low permeability of the reservoir.

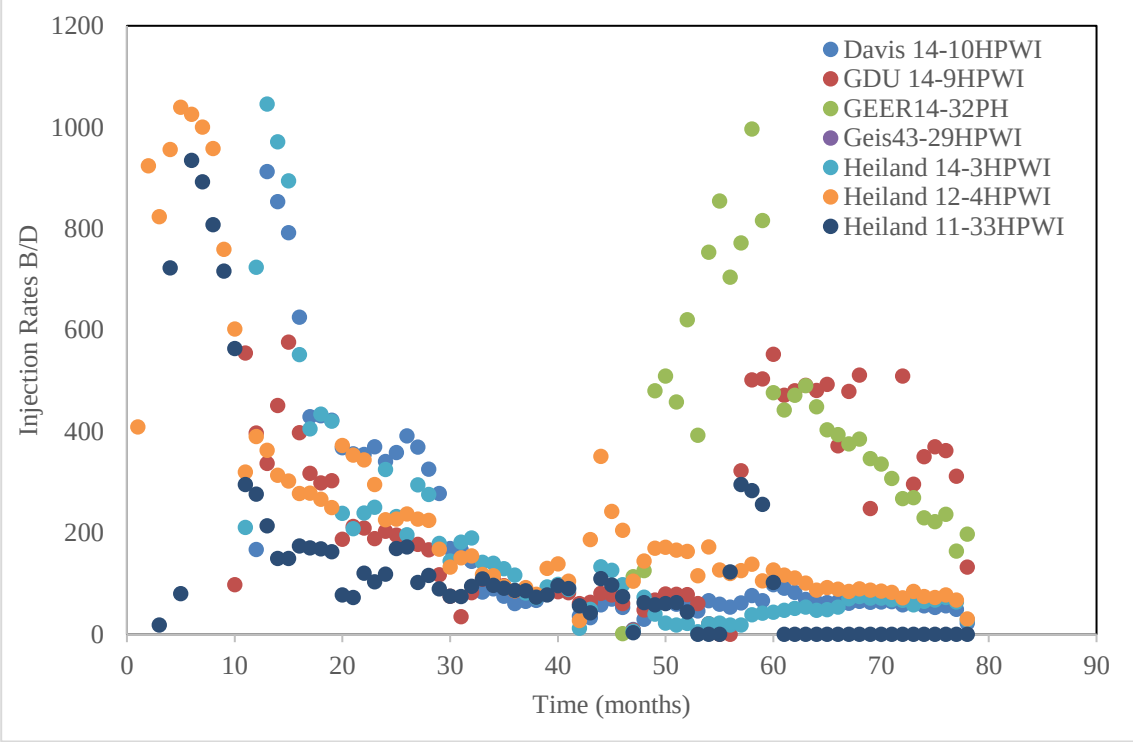

Figure 4-5 —Injection rates for all the injectors in 21 Mile Butte and Gaither Draw Unit.

The bubble maps shown in Figure 4-6 and Figure 4-7 indicate the relative contributions of the cumulative oil and water productions from each well. The shaded

area with green, pink and brown represent the 21 Mile Butte, Gaither Draw Unit and South Gaither, respectively.

The largest bubble in Figure 4-7 is well GDU 44-8PH with cumulative water production of 260,000 bbls. From the figures, it can be noticed that 21 Mile Butte recovered more oil, while water was mainly produced from the south part of the Gaither Draw Units, particularly in South Gaither. Also, horizontal wells produced more fluid than vertical wells in the same area. Figure 4-8 shows the water cut of six horizontal wells from three sections. GDU 12-5HP and GDU 13-35HP are two typical horizontal producers from Gaither Draw Unit. Heiland Trust 14-31PH and Heyden 14-1PH are from 21 Mile Butte, and Davis 13-15PH and Davis State 43-16PH are representing South Gaither Draw.

Figure 4-8 shows that South Gaiter has the higher water cut compared to with 21 Mile Butte and Gaither Draw Unit. For the wells in 21 Mile Butte, the water cut remains around 30% for almost 30 months, suggesting they are the most valuable and productive wells. The information from Figure 4-8 is corresponding with previous two figures.

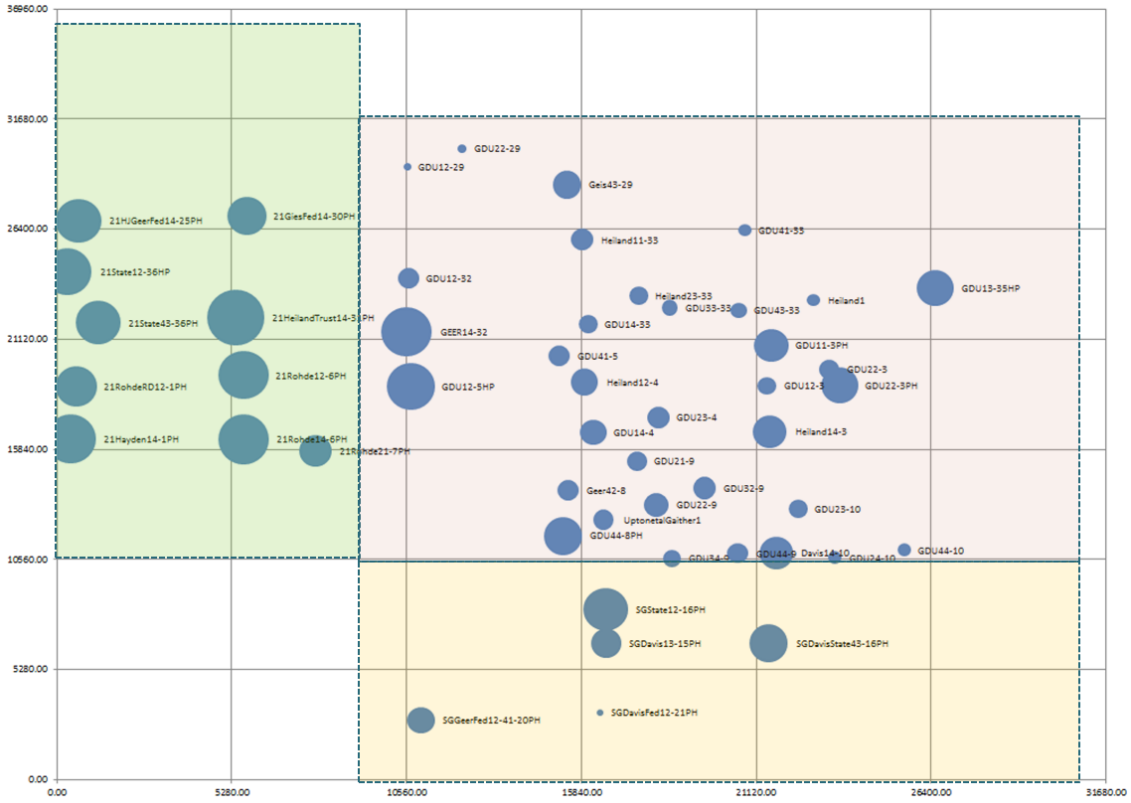

Figure 4-6 —Cumulative oil production map; circle size is proportional to the amount of cumulative oil production.

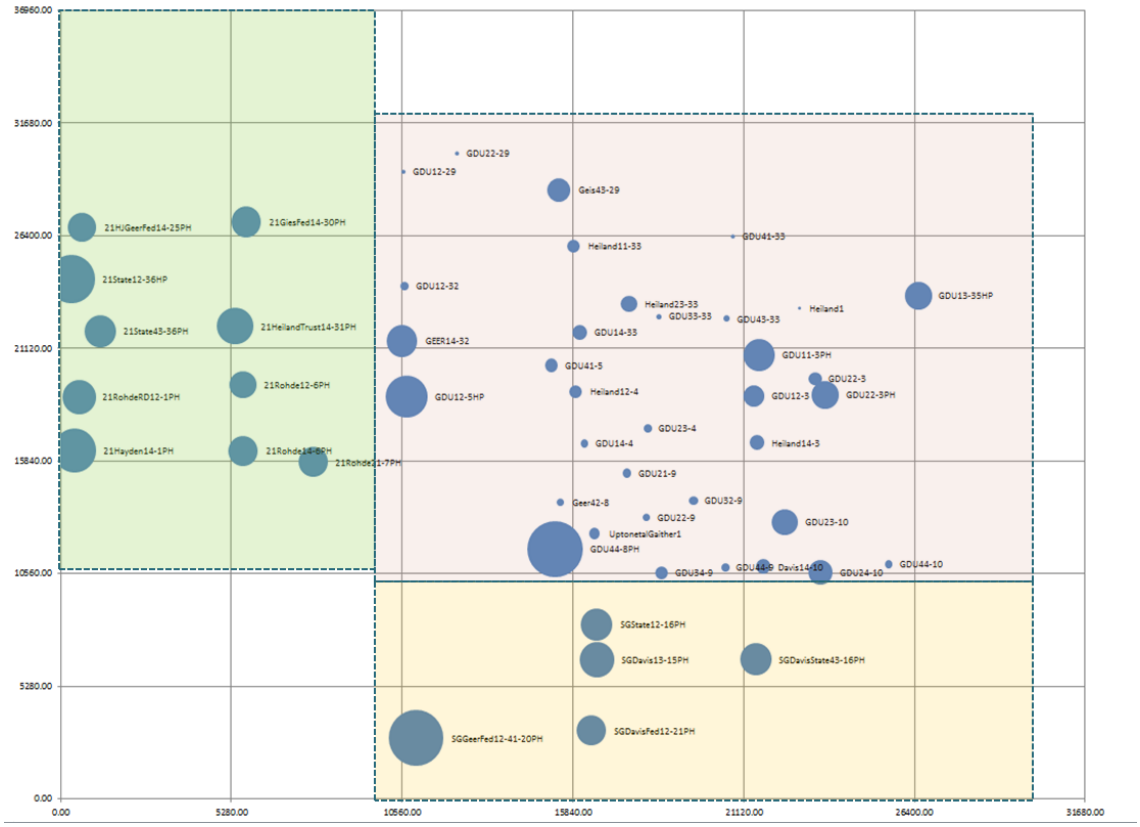

Figure 4-7 —Cumulative water production map; circle size is proportional to the amount of cumulative water production.

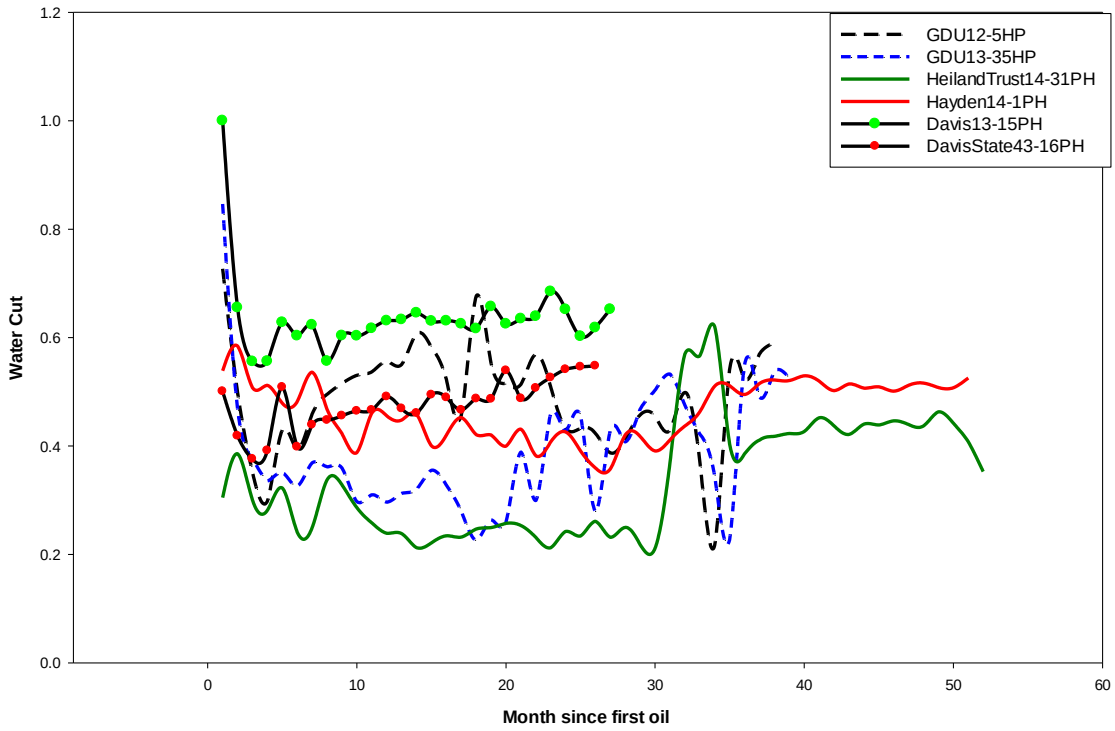

Figure 4-8 —The water cut from typical wells.

4.3 Selection of Data and Analysis Area

There are 50 production wells in the field. For the CRM analysis, it is important to consider how many data points are available. With more injection and production data, more accurate information about the reservoir properties can be determined from the CRM analysis.

Based on the injection/production data, the recorded well activity period is from June of 2007 to January of 2017. In the analysis, the monthly production data was used to determine the unknown parameters in the CRM model. Therefore, there are 116 data points available that can be used on the CRM model to obtain weights and the time constant without considering later well activity transfer of special wells.

However, assuming all wells begin operating at the same time and continue operating until January of 2017, there are 50 production wells and 7 injection wells. With assuming constant bottom hole pressure, there are 357 unknown weights and 357 unknown time constants in this system. Therefore, in total, there are 714 unknown parameters in the CRMIP that require estimation. At least 714 data points are required to solve this problem and determine the 714 unknown parameters. The existing 116 data points is not enough to determine all 714 parameters by CRMIP approach.

With the CRMP approach, the number of unknown parameters is reduced to 408. However, the available 116 data points is still insufficient. Due to the low permeability and high heterogeneity of this reservoir, the assumption that each injection well is only connected with the surrounding producers is valid. On the basis of this assumption, the whole field can be divided into seven zones to conduct the CRM analysis (Figure 4-10).

4.4 Results and Discussions

In region 1, the injection well named GDU 14-9HPWI is surrounded by eight production wells, GDU 21-9, GEER 42-8, GDU 44-8PH, UPTONETAL GAITHER 1, GDU 22-9, GDU 32-9, GDU 34-9, SG STATE 12-16PH. The relative positions of these wells are shown in Figure 4-11. Since only part of the field was chosen to analyze, the unbalanced capacitance model (UCM) approach should be used. The constant term can account for the flow across the boundary of the selected area and unbalanced condition of the field injection and production rates.

For the CRM analysis, the transient flow period should be avoided. The time lag between injectors and producers is due to compressibility rather than time of pressure transferring from injectors to producers. In this case, the period selected is from April 2015 to January 2017. Therefore, 22 data points with 24 unknown parameters should be obtained, which would give a much more reasonable result than conducting the CRM analysis in the whole field. Figure 4-12 shows the injection and production data for region 1, from April 2015 to January 2017.

By using the solver given in section 3.3 and inputting selected injection and production data, eight weights, eight time constants and eight constant coefficients can be calculated. In this case, the objective function is set to the difference between calculated and real production rates. Table 4.2 shows the results of the weights and constant coefficients. **Error! Reference source not found.** shows the results of the time constant. Figure 4-13 to Figure 4-14 show typical fitting results for production rates of region 1.

From the results of interwell connectivity and the time constant in region 1, one can conclude that there is a high connection between UPTONETAL GAITHER 1 and GDU 14-9HPWI. Also, Figure 4-12 indicates that UPTONETAL GAITHER 1 has highest production rates among 8 producers and the relation between UPTONETAL GAITHER 1 is obvious.

For most regions, the time constant between each injector/producer pair is large. That means the storage effect of the reservoir medium is so strong that most injected water just saturated around the injector. It shows the same characters as CMG full field model presents. The input for CMG simulation is available upon request. Figure 4-9 shows water saturation profile at the end of the simulation. The results for region 2 to region 7 are shown from Figure 4-15 to Figure 4-38.

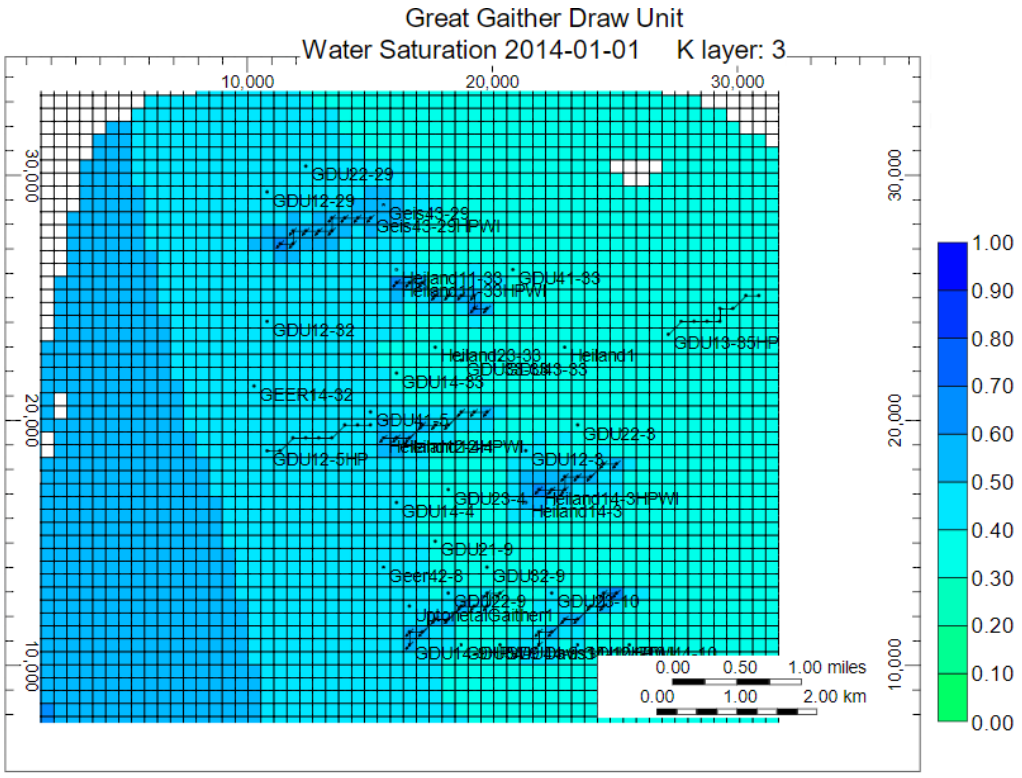

Figure 4-9 —Water saturation profile at the end of the simulation

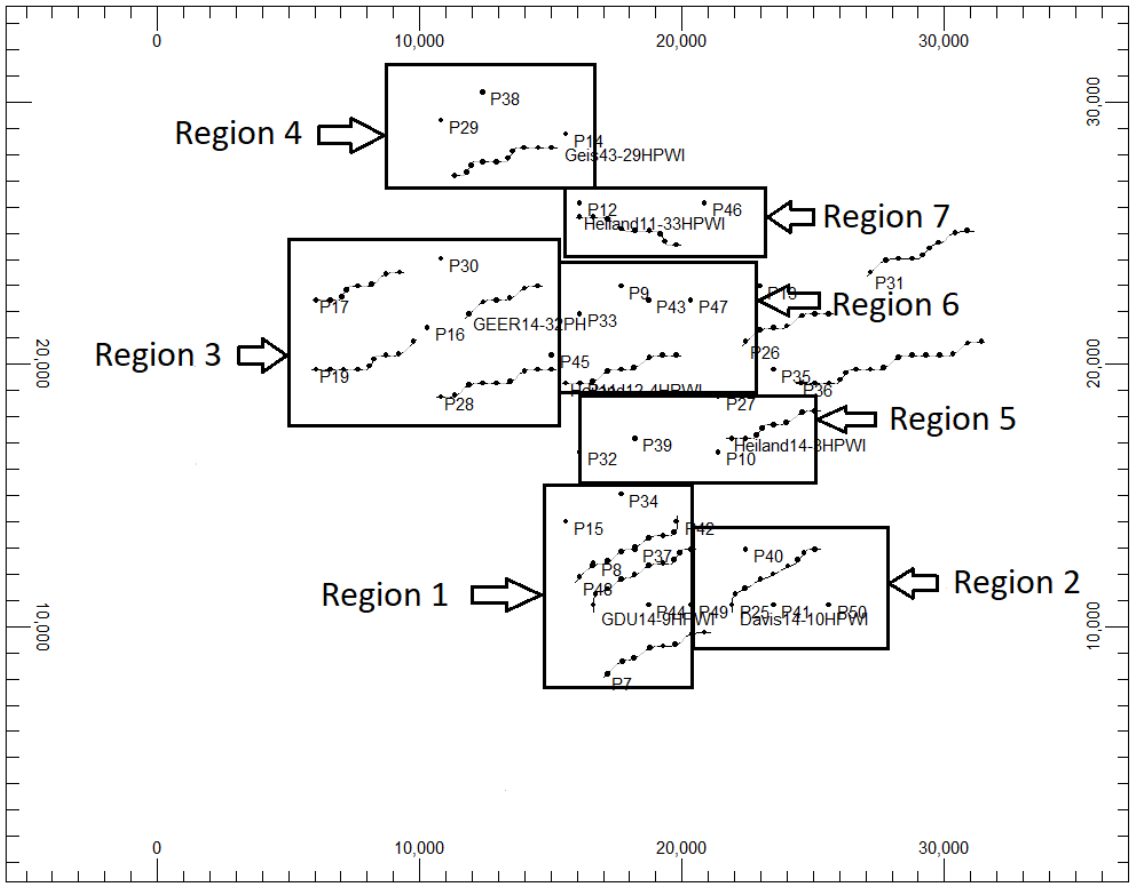

Figure 4-10 —The field is divided into seven zones to conduct the CRM analysis.

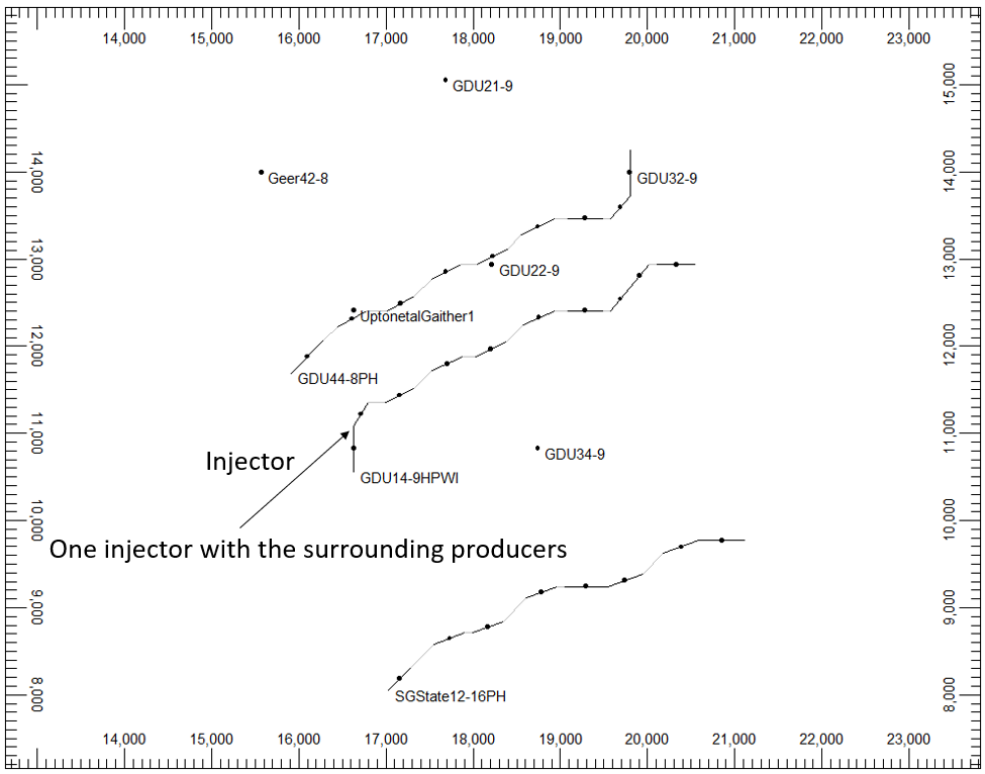

Figure 4-11 —Relative well positions for region 1. Injection well: GDU 14-9HPWI.

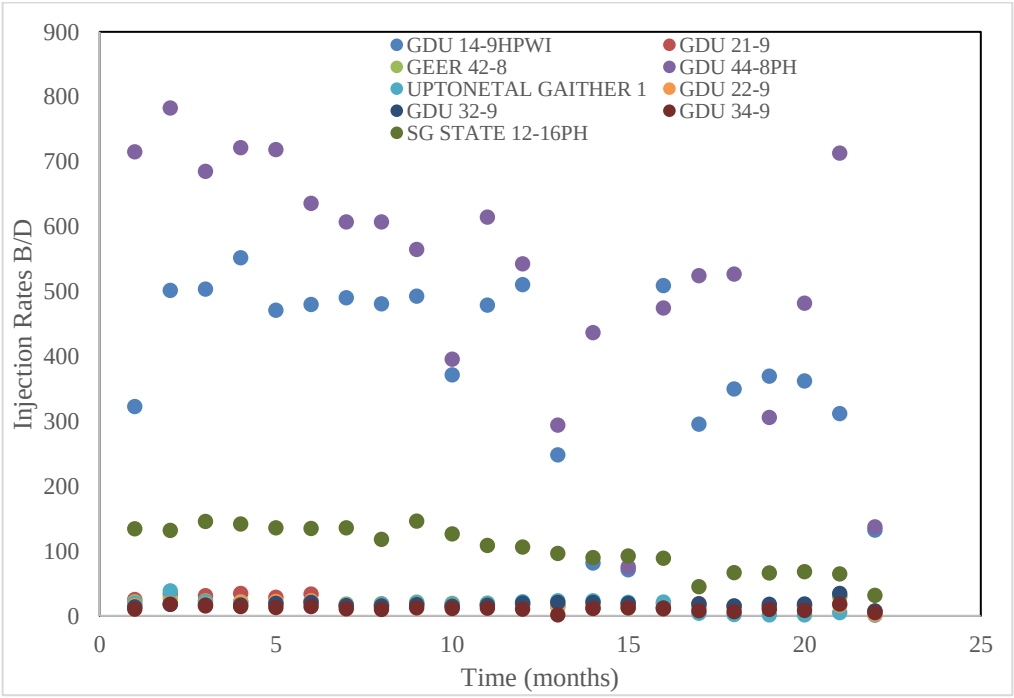

Figure 4-12 —Injection and production data during the analyzing period of region 1.

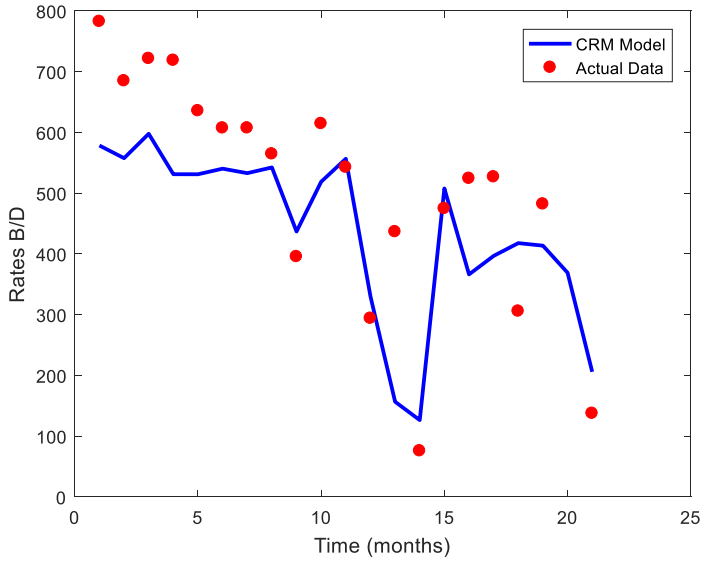

Figure 4-13 —Fitting result of GDU 44-8PH. Red dots indicate the actual production rates. Blue line indicates the production rates calculated with the estimated parameters.

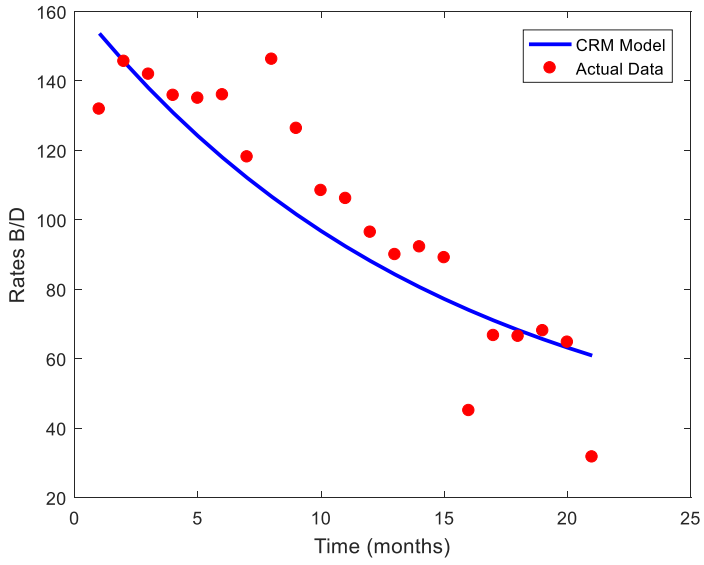

Figure 4-14 —Fitting result of SG STATE 12-16PH. Red dots indicate the actual production rates. Blue line indicates the production rates calculated with the estimated parameters.

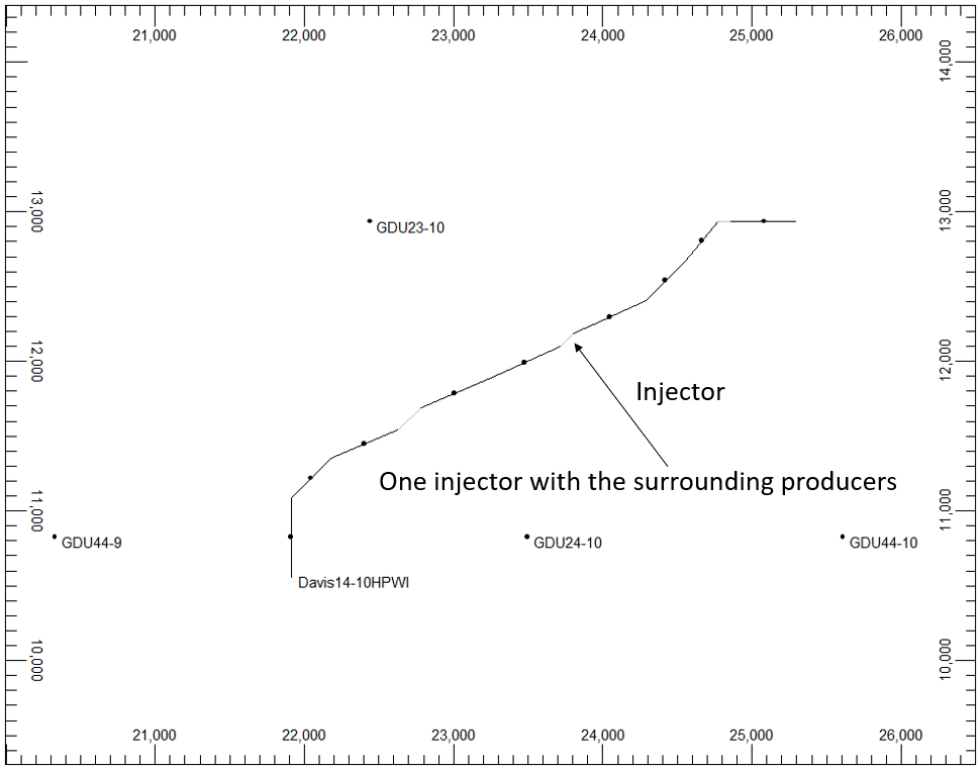

Figure 4-15 —Relative well positions for region 2. Injection well: Davis 14-10HPWI.

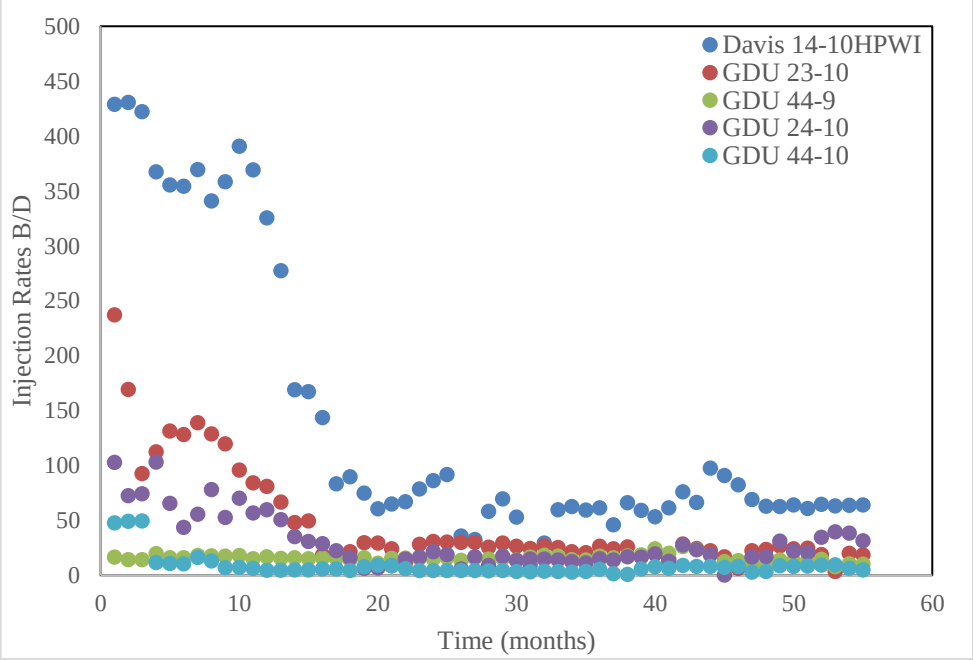

Figure 4-16 —Injection and production data during the analyzing period of region 2.

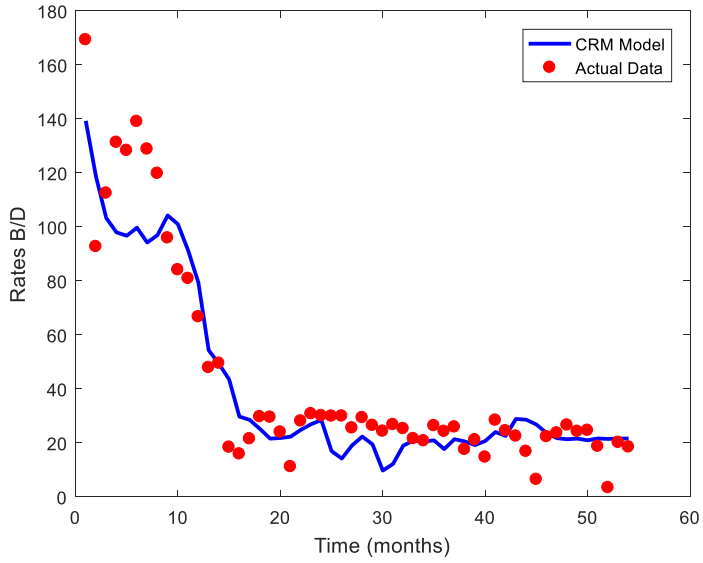

Figure 4-17 —Fitting result of GDU 23-10. Red dots indicate the actual production rates. Blue line indicates the production rates calculated with the estimated parameters.

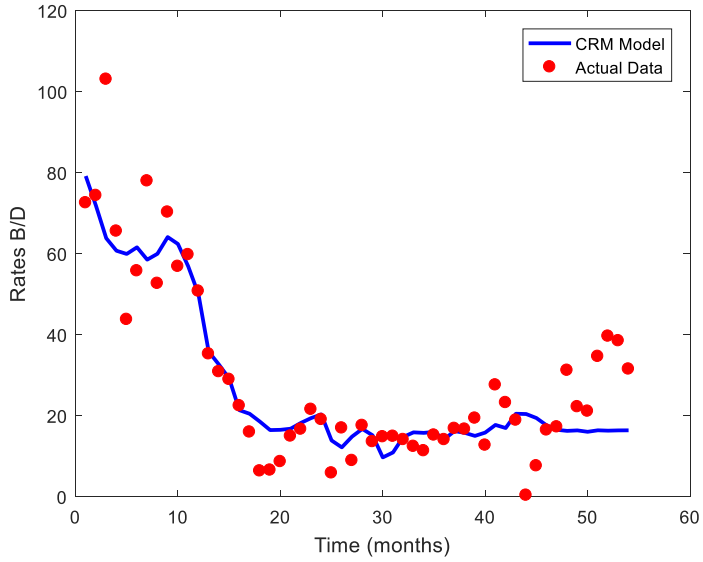

Figure 4-18 —Fitting result of GDU 24-10. Red dots indicate the actual production rates. Blue line indicates the production rates calculated with the estimated parameters.

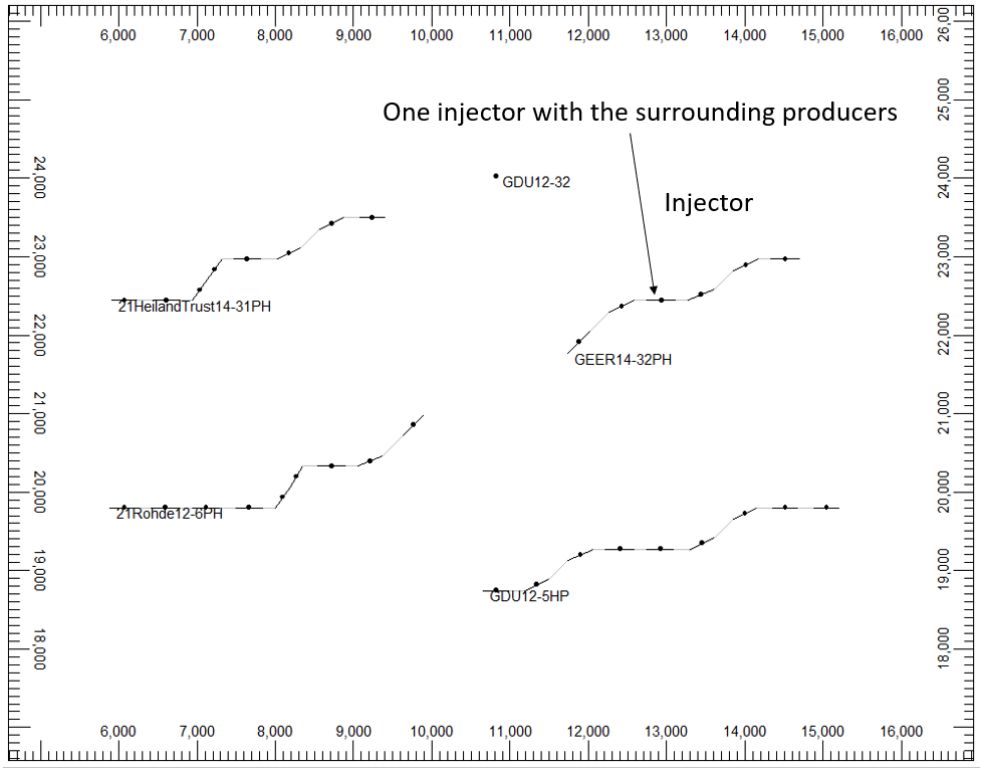

Figure 4-19 —Relative well positions for region 3. Injection well: Geer 14-32PH.

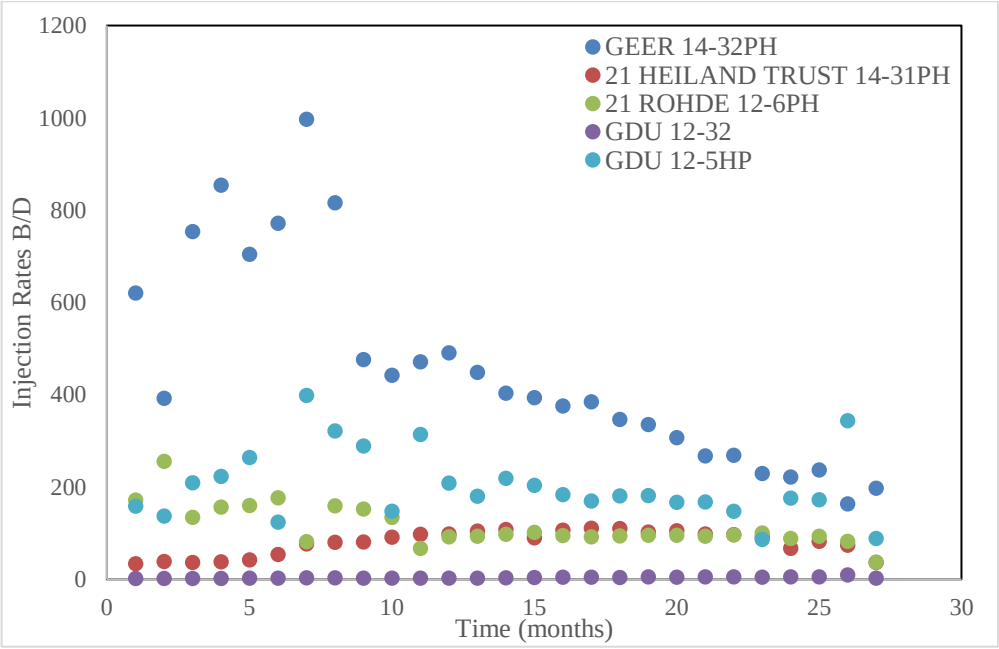

Figure 4-20 —Injection and production data during the analyzing period of region 3.

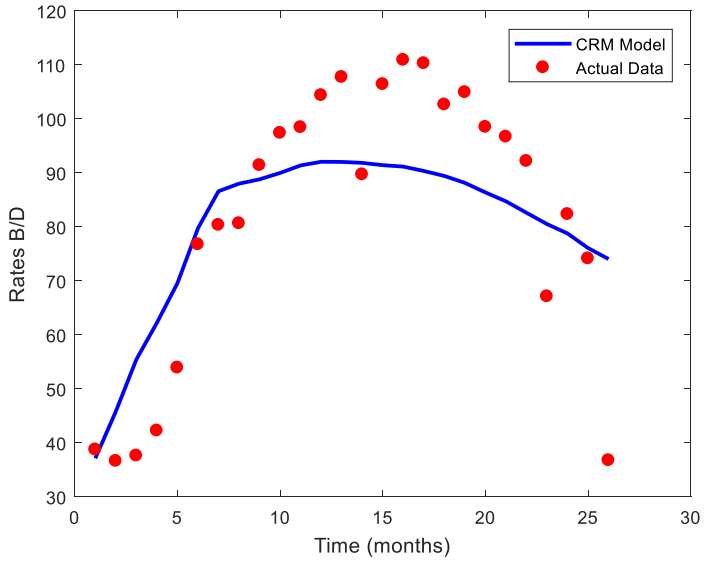

Figure 4-21 —Fitting result of 21 Heiland Trust 14-31PH. Red dots indicate the actual production rates. Blue line indicates the production rates calculated with the estimated parameters.

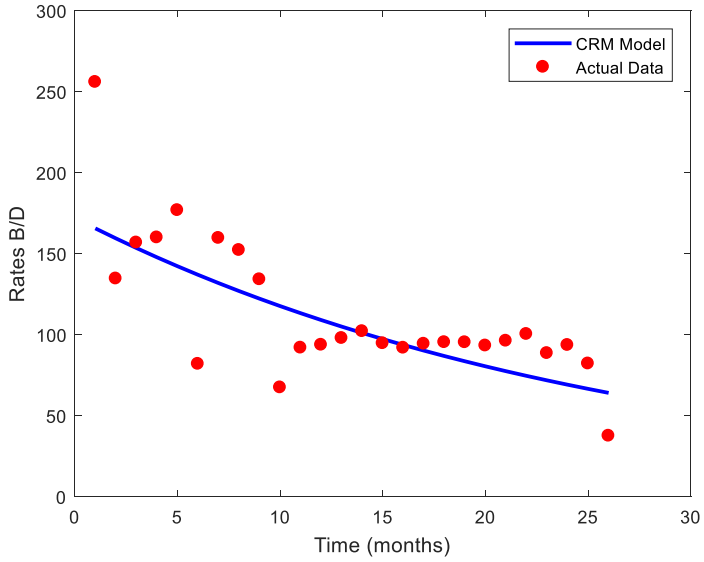

Figure 4-22 —Fitting result of 21 ROHDE 12-6PH. Red dots indicate the actual production rates. Blue line indicates the production rates calculated with the estimated parameters.

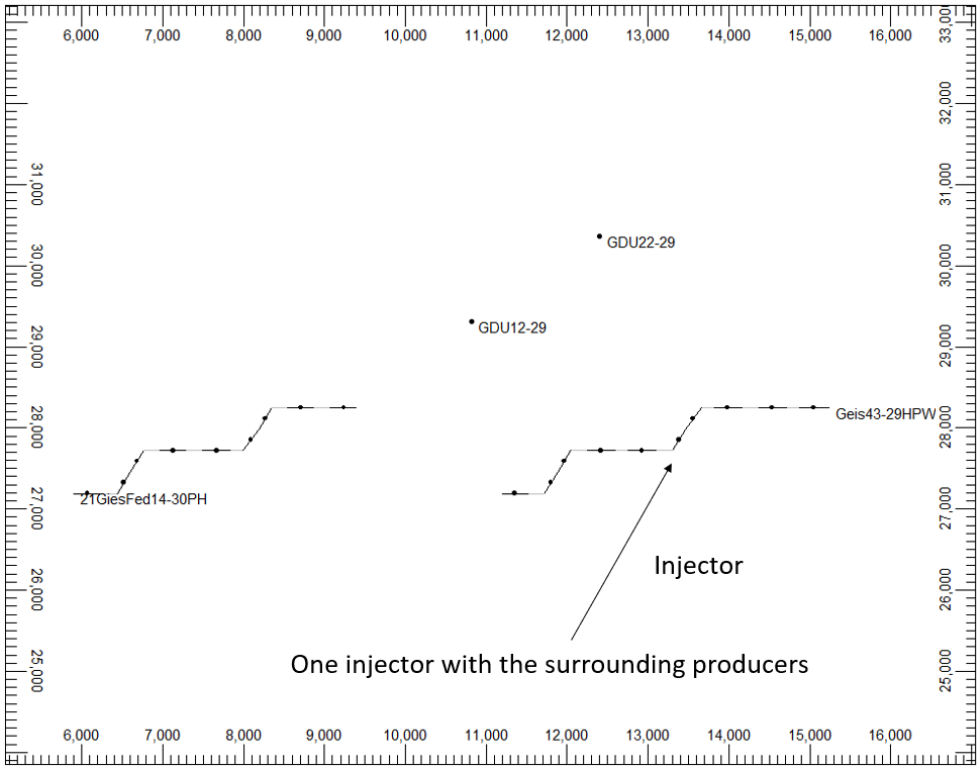

Figure 4-23 —Relative well positions for region 4. Injection well: Geis 43-29HPWI.

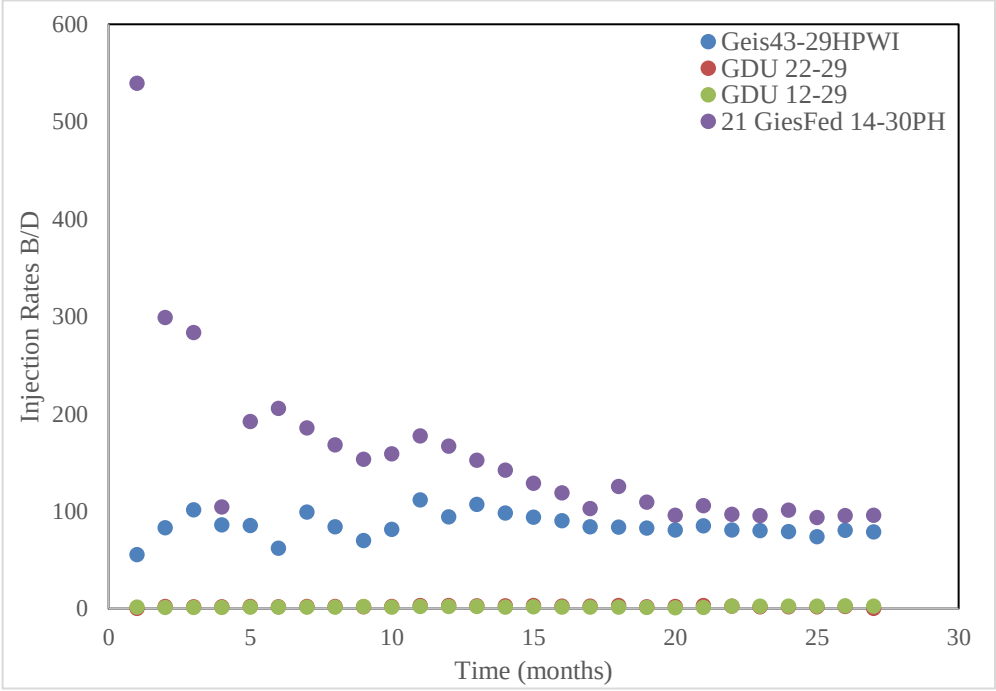

Figure 4-24 —Injection and production data during the analyzing period of region 4.

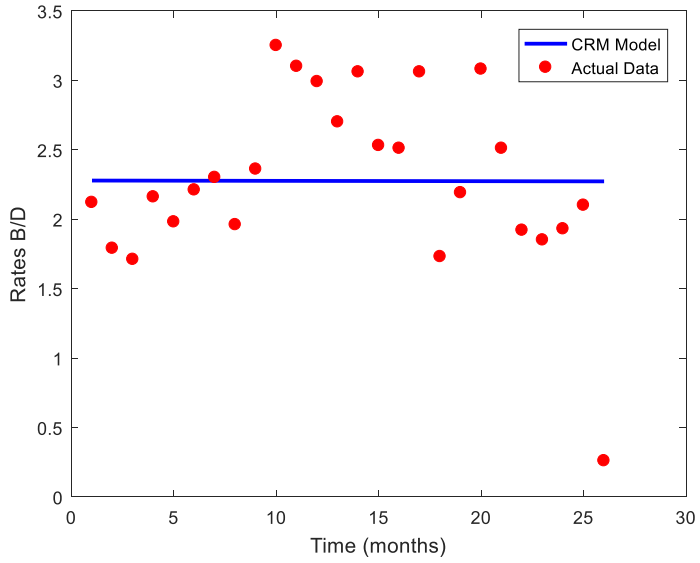

Figure 4-25 —Fitting result of GDU 22-29. Red dots indicate the actual production rates. Blue line indicates the production rates calculated with the estimated parameters.

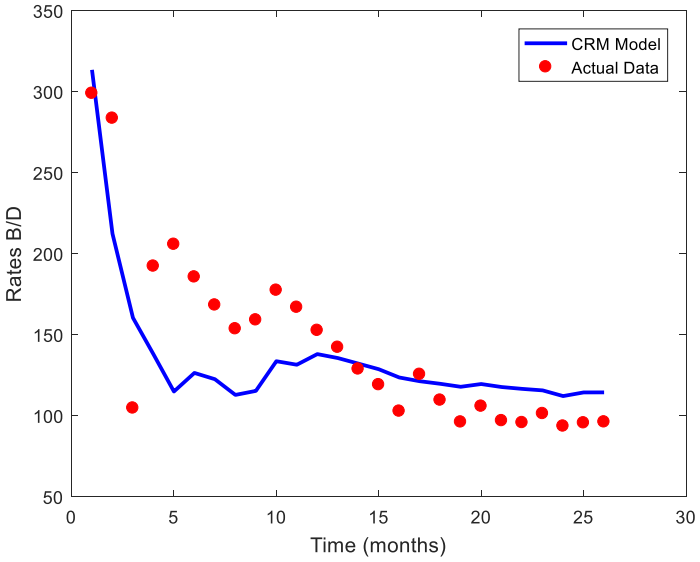

Figure 4-26 —Fitting result of 21 GiesFed 14-30PH. Red dots indicate the actual production rates. Blue line indicates the production rates calculated with the estimated parameters.

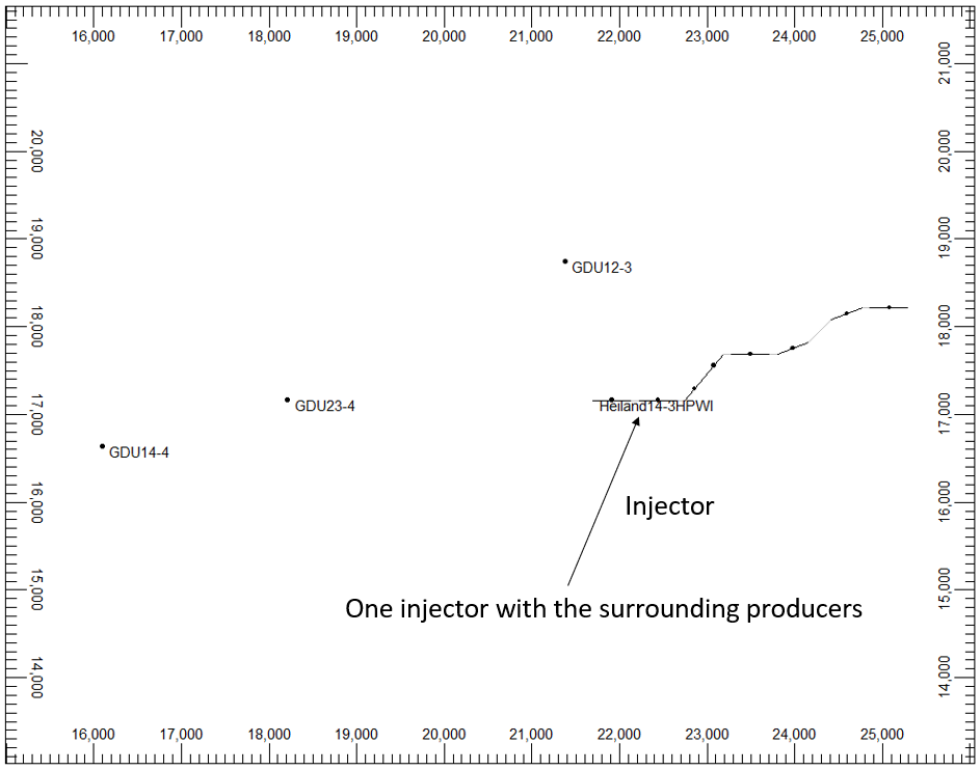

Figure 4-27 —Relative well positions for region 5. Injection well: Heiland 14-3HPWI.

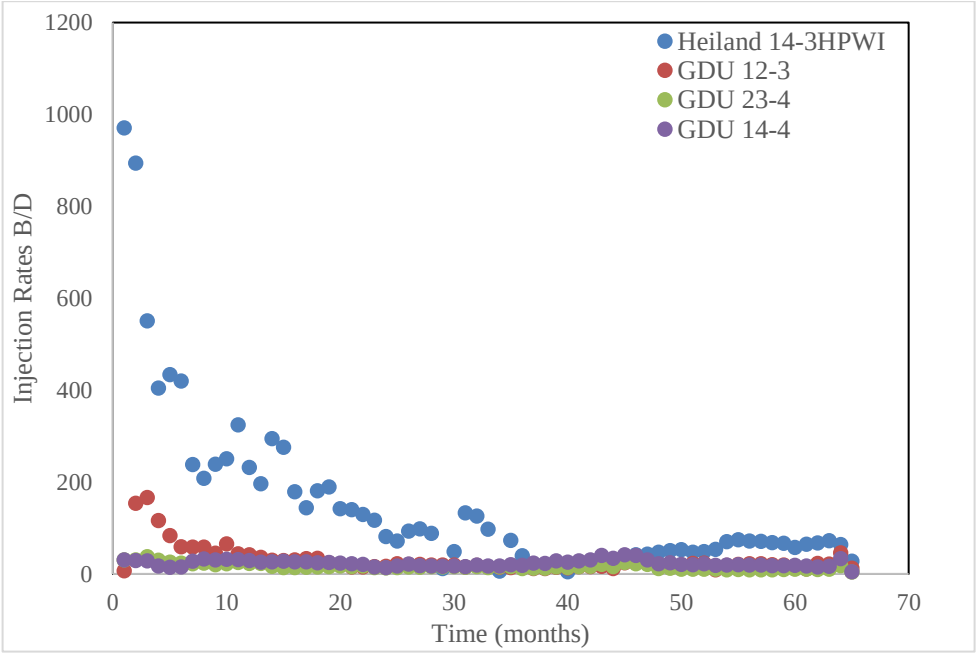

Figure 4-28 —Injection and production data during the analyzing period of region 5.

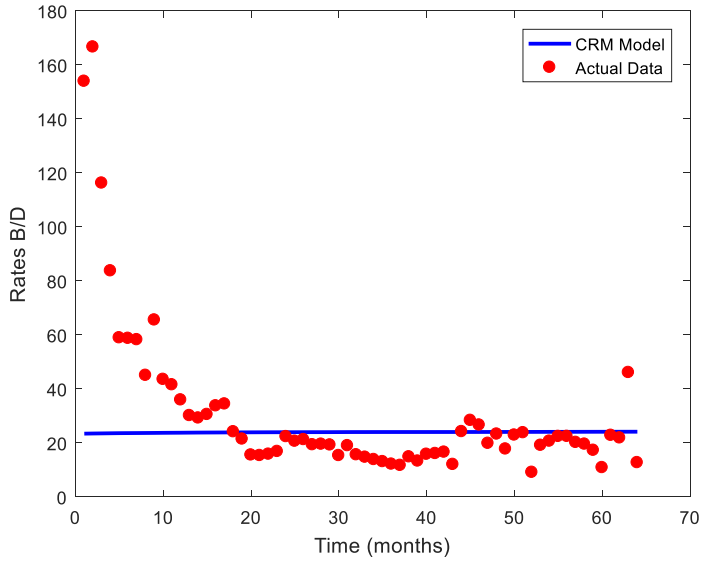

Figure 4-29 —Fitting result of GDU 12-3. Red dots indicate the actual production rates. Blue line indicates the production rates calculated with the estimated parameters.

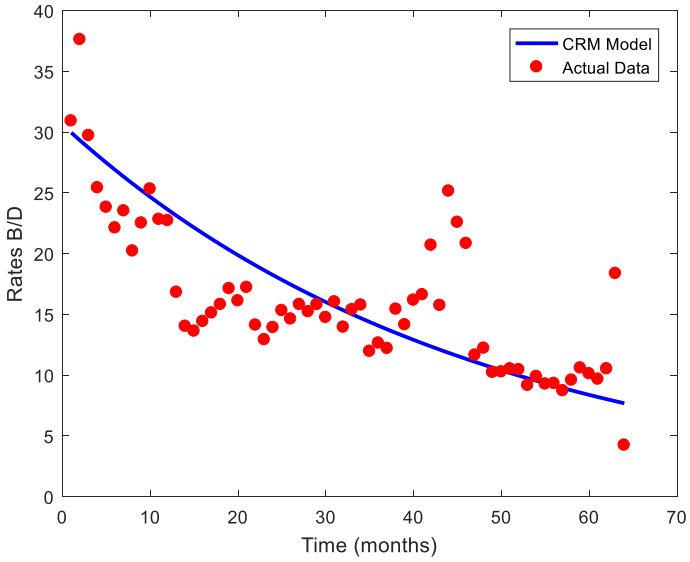

Figure 4-30 —Fitting result of GDU 23-4. Red dots indicate the actual production rates. Blue line indicates the production rates calculated with the estimated parameters.

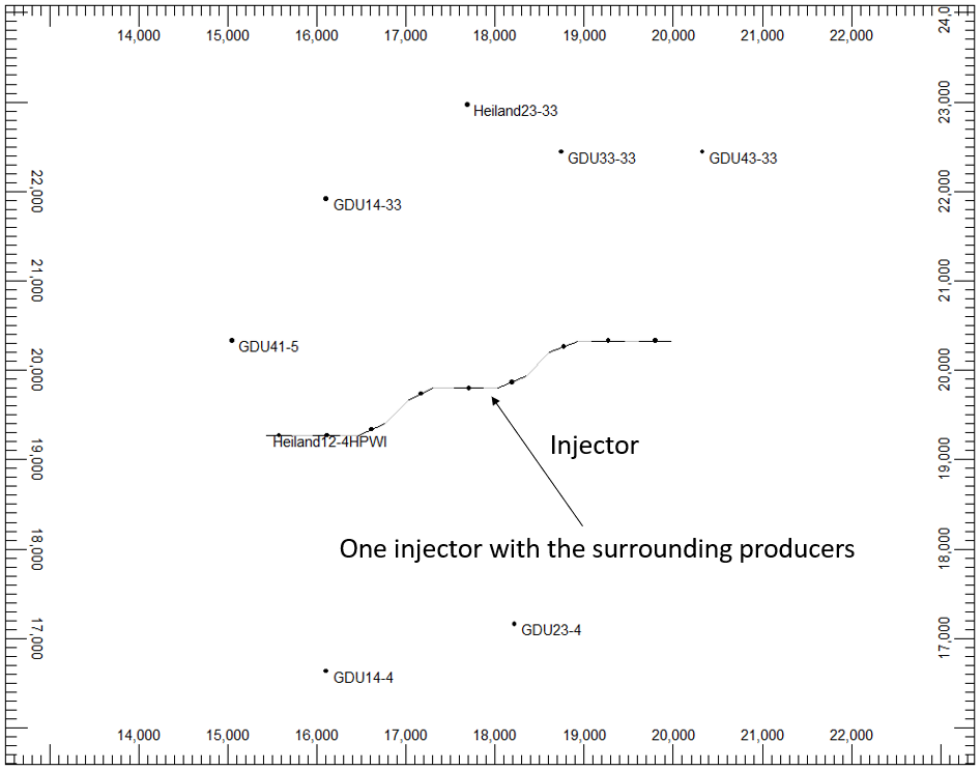

Figure 4-31 —Relative well positions for region 6. Injection well: Heiland 12-4HPWI.

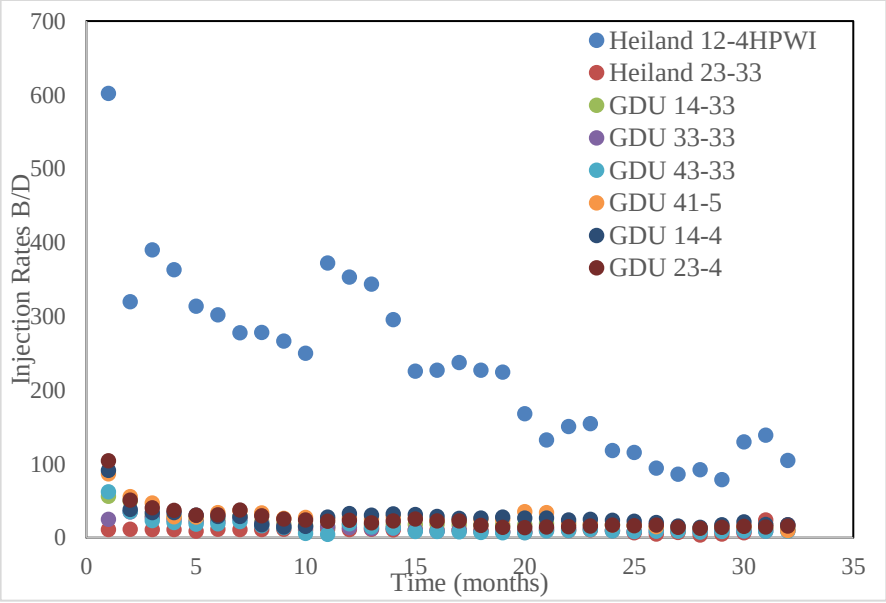

Figure 4-32 —Injection and production data during the analyzing period of region 6.

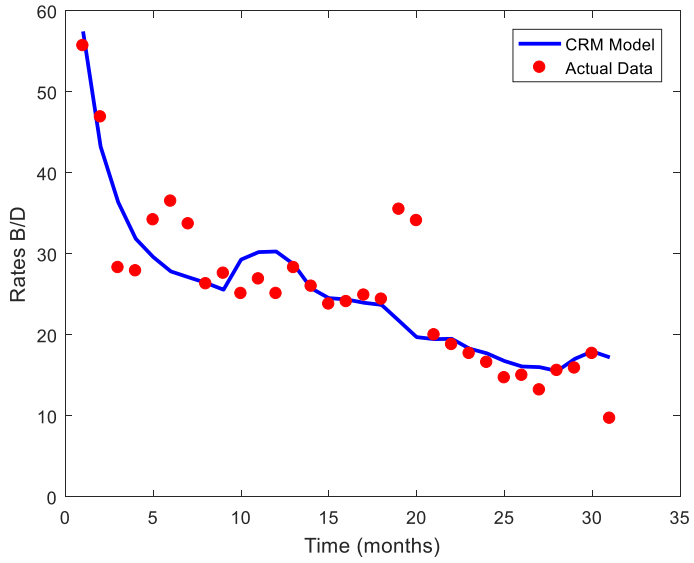

Figure 4-33 —Fitting result of GDU 41-5. Red dots indicate the actual production rates. Blue line indicates the production rates calculated with the estimated parameters.

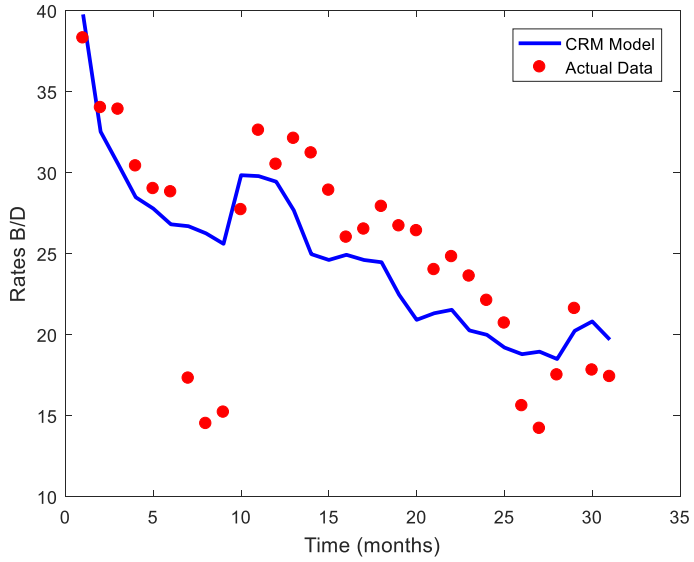

Figure 4-34 —Fitting result of GDU 14-4. Red dots indicate the actual production rates. Blue line indicates the production rates calculated with the estimated parameters.

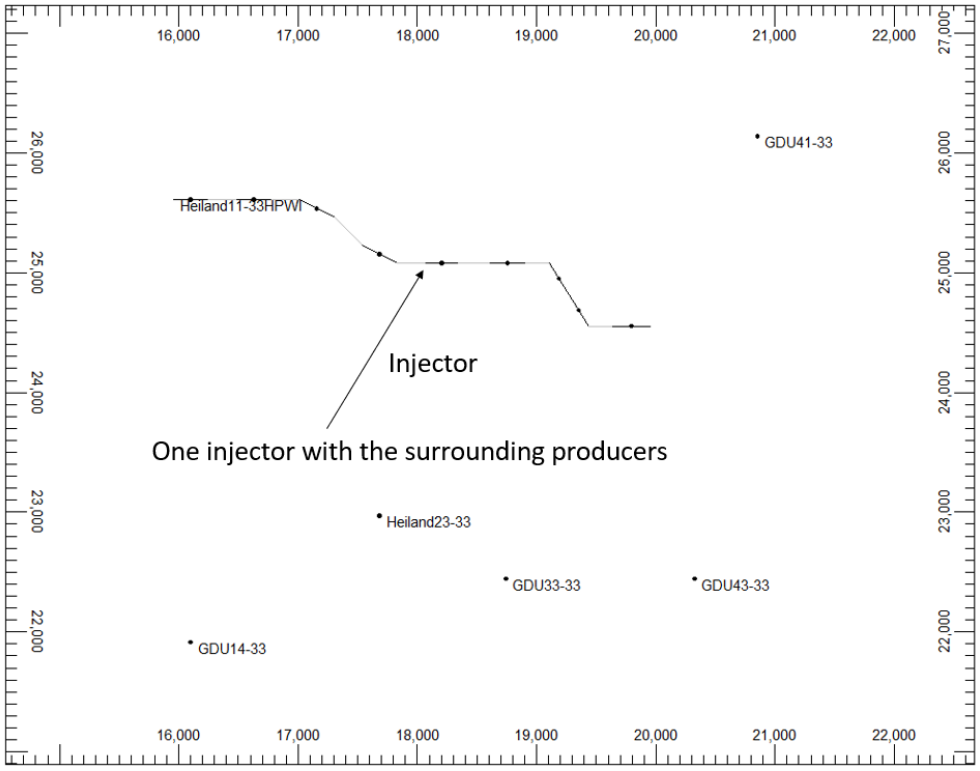

Figure 4-35 —Relative well positions for region 7. Injection well: Heiland 11-33HPWI.

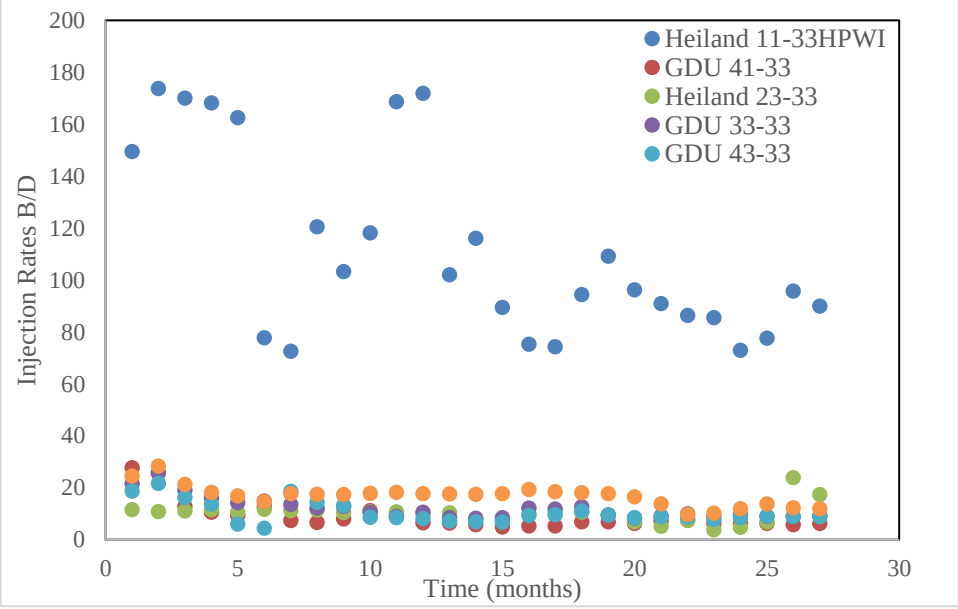

Figure 4-36 —Injection and production data during the analyzing period of region 7.

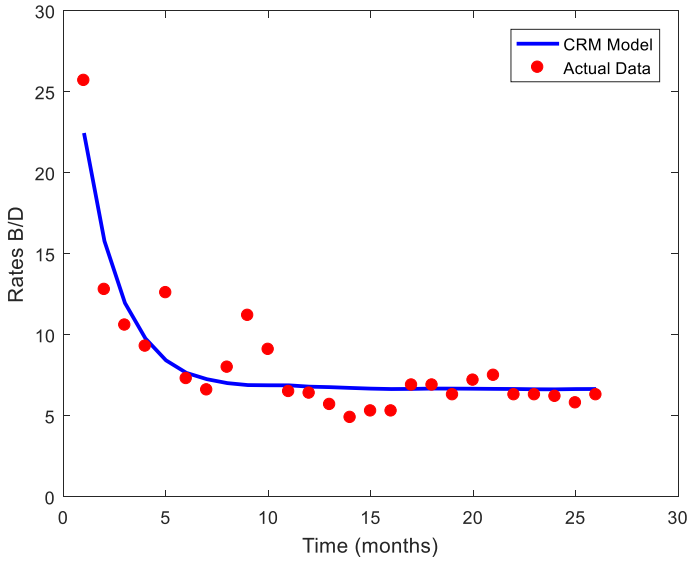

Figure 4-37 —Fitting result of GDU 41-33. Red dots indicate the actual production rates. Blue line indicates the production rates calculated with the estimated parameters.

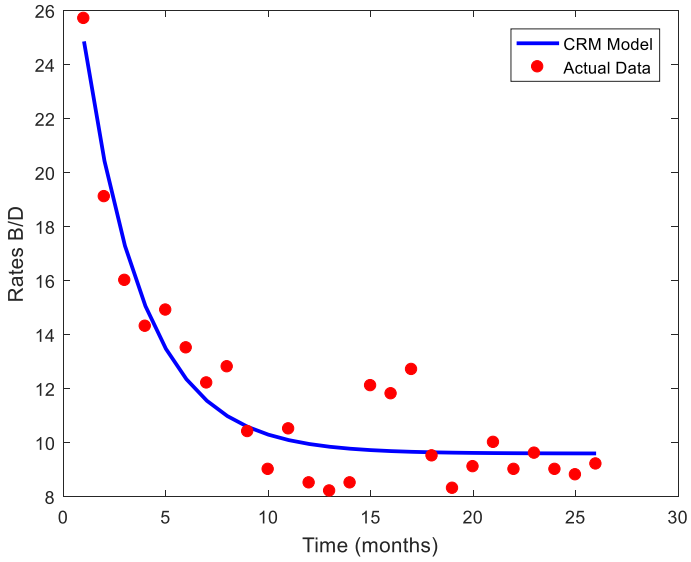

Figure 4-38 —Fitting result of GDU 33-33. Red dots indicate the actual production rates. Blue line indicates the production rates calculated with the estimated parameters.

Table 4.2 —Region 1 weights, time constant and constant coefficients.

	Connectivity	Time Constant	Constant coefficient
GDU 21-9	0.00	4.34	15.49
GEER 42-8	0.00	29.36	2.33
GDU 44-8PH	1.00	0.47	51.11
UPTONETAL GAITHER 1	0.00	11.31	6.82
GDU 22-9	0.00	19.35	6.42
GDU 32-9	0.00	1107.26	3.88
GDU 34-9	0.00	4.55	9.07
SG STATE 12-16PH	0.00	14.93	27.95

Table 4.3 —Region 2 weights, time constant and constant coefficients.

	Connectivity	Time constant	Constant coefficient
GDU 23-10	0.26	0.59	5.18
GDU 44-9	0.59	10000.00	0.00
GDU 24-10	0.15	0.64	6.82
GDU 44-10	0.00	2.80	5.50

Table 4.4 —Region 3 weights, time constant and constant coefficients.

	Connectivity	Time constant	Constant coefficient
21 HEILAND TRUST 14-31PH	0.23	14.90	0.00
21 ROHDE 12-6PH	0.00	26.30	0.00
GDU 12-32	0.40	1652.26	0.00
GDU 12-5HP	0.37	7.68	1.16

Table 4.5 —Region 4 weights, time constant and constant coefficients.

	Connectivity	Time constant	Constant coefficient
GDU 22-29	0.00	805.36	2.09
GDU 12-29	0.00	9995.66	0.34
21 GiesFed 14-30PH	1.00	1.17	35.64

Table 4.6 —Region 5 weights, time constant and constant coefficients.

	Connectivity	Time constant	Constant coefficient
GDU 12-3	1.00	10000.00	16.26
GDU 23-4	0.00	46.27	0.00
GDU 14-4	0.00	120.50	0.00

Table 4.7 —Region 6 weights, time constant and constant coefficients.

	Connectivity	Time constant	Constant coefficient
Heiland 23-33	0.80	10000.00	0.00
GDU 14-33	0.02	1.79	11.04
GDU 33-33	0.00	6.86	8.80
GDU 43-33	0.02	1.34	5.46
GDU 41-5	0.06	1.15	10.71
GDU 14-4	0.04	0.52	15.16
GDU 23-4	0.05	0.99	8.36

Table 4.8 —Region 7 weights, time constant and constant coefficients.

	Connectivity	Time constant	Constant coefficient
GDU 41-33	0.00	1.79	6.43
Heiland 23-33	1.00	10000.00	0.00
GDU 33-33	0.00	2.92	9.59
GDU 43-33	0.00	1.87	8.92
GDU 14-33	0.00	34.56	0.00

Chapter 5 Production Forecast from CRM for the Studied Field

The CRM model can be used in a predictive mode to forecast production rates for each producer. After the weights and time constant are determined during the training period, the liquid production rates for each producer can be predicted by inputting future injection rates.

For Gaither Draw Units, the well performance since January of 2017 is forecasted and compared with numerical simulation results. The production rates to December 2019 are predicted by using the CRM model and CMG full field model separately. The full field model is obtained by history matching in CMG, a finite difference simulator. For the full field model, since the pressure date for producers/injectors at the bottom-hole were absent when the model was being built, the liquid daily rate is set up as the producer constraint to achieve history match on rates. The permeability field for the full field model was generated using Sequential Gaussian Simulation. In this process, the average permeability of Gaither Draw Units and South Gaither sections is assumed to be 0.1 md, while the average permeability of 21 Mile Butte section is assumed to be 1md, since this area has better production performance. The entire permeability field follows a log-normal distribution with standard derivation of 2 to reflect the heterogeneity of the reservoir. The injection rates, which are required to predict the production rates are set according to the last month of available data. The typical injection rates for prediction are shown in Figure 5-1. The predicted production rates of both the CRM model and CMG full field model are shown and compared from Figure 5-2 to Figure 5-6.

For the producer benefitting from the injection, which means relative large weight and small time constant between the injector/producer pair, the predicted production rates

of the CRM model will remain constant due to the constant injection rates during the prediction period. However, for the CMG full field model, the producers are constrained by the total liquid rate regardless of bottom hole pressure. To achieve history match on rates, local permeability is changed for some producers. The permeability for interwell blocks remain unchanged in the history matching process. The CMG full filed model does not focus on interwell region and the history match of rates is mainly due to the changing bottom hole pressure. In the prediction process, the bottom hole pressure is set according to the last month of available data. The predicted production rates of the CMG full field model show a sharp decrease, and the producer may even stop producing, as shown from Figure 5-4 to Figure 5-6.

For the producer not benefitting from the injection, which means relative small weight and large time constant, the production rates are mainly associated with the primary production rates. The decline rate is small due to large time constant. The predicted production rates of the CRM model and CMG full field model agree, as shown in Figure 5-3.

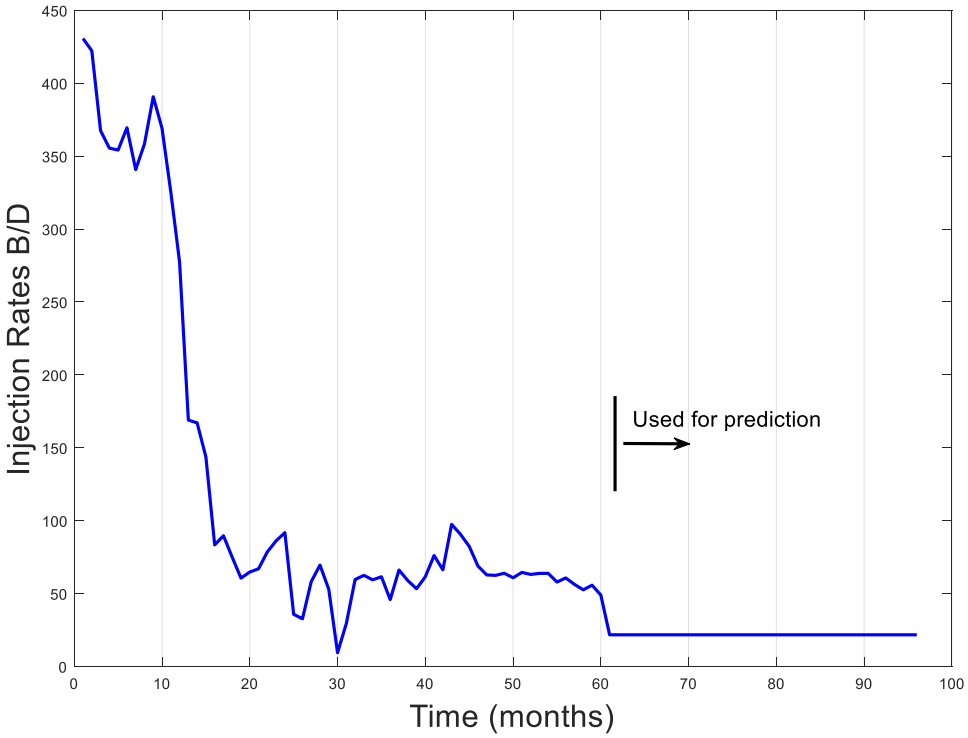

Figure 5-1—Injection rates for Davis 14-10HPWI.

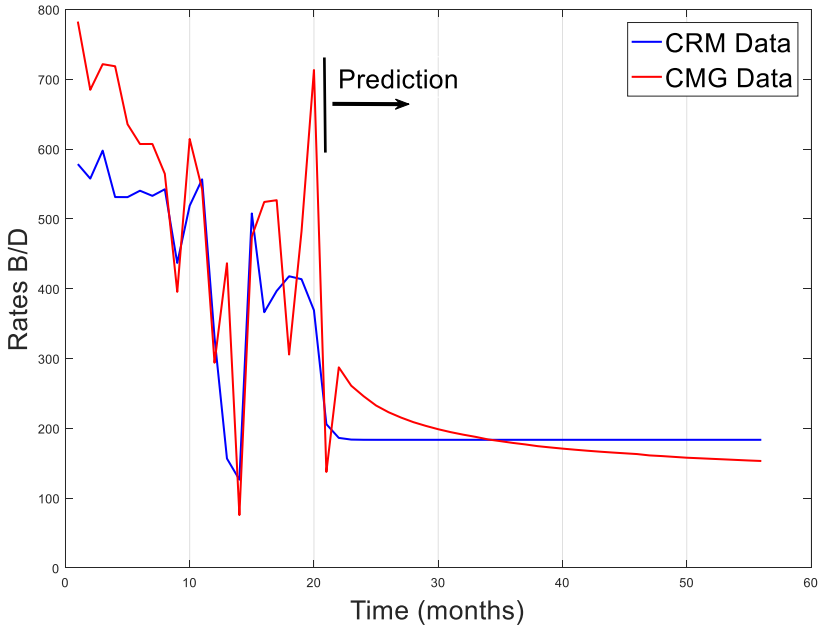

Figure 5-2 —Predicted production of GDU 44-8 PH. Red dots indicate the CRM prediction. Blue line indicates the CMG prediction.

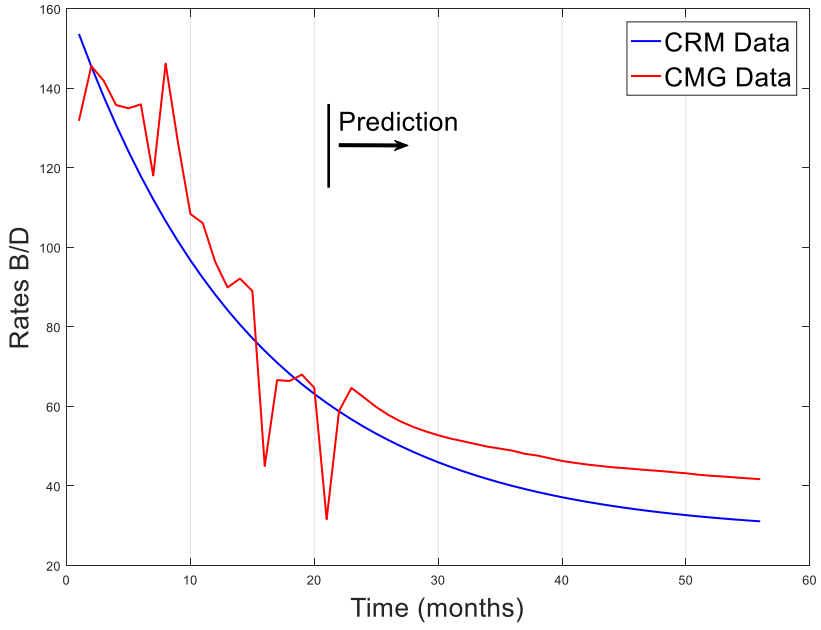

Figure 5-3 —Predicted production of SG STATE 12-16PH. Red dots indicate the CRM prediction. Blue line indicates the CMG prediction.

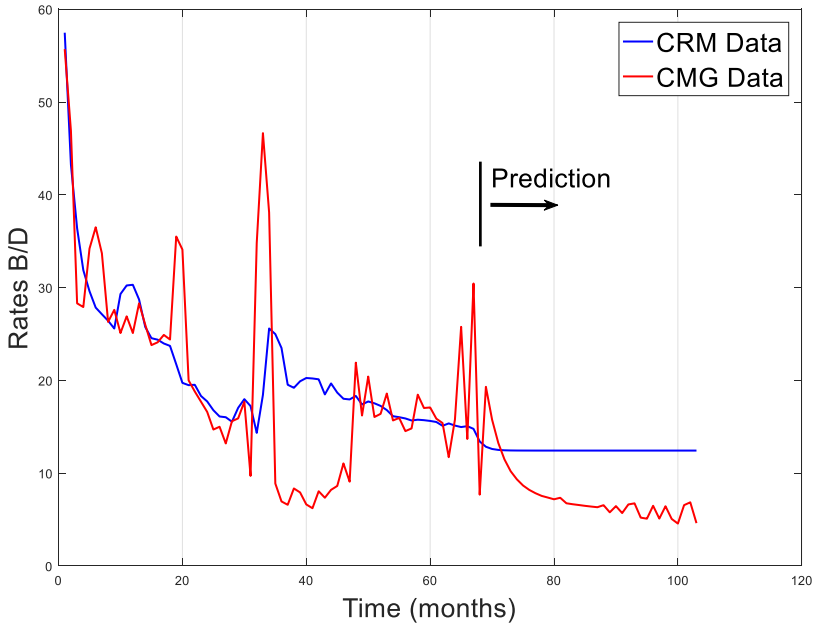

Figure 5-4 —Predicted production of GDU 41-5. Red dots indicate the CRM prediction. Blue line indicates the CMG prediction.

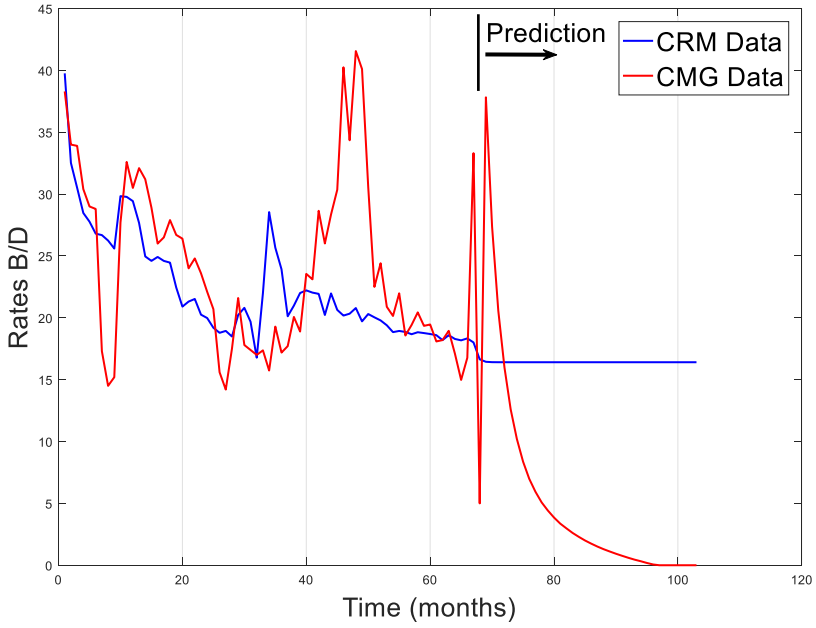

Figure 5-5 —Predicted production of GDU 14-4 PH. Red dots indicate the CRM prediction. Blue line indicates the CMG prediction.

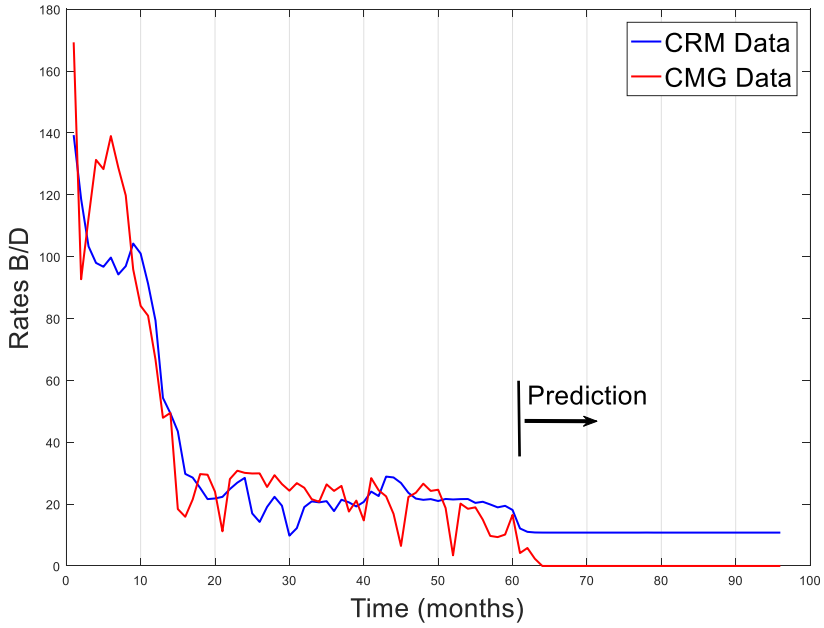

Figure 5-6 —Predicted production of GDU 23-10. Red dots indicate the CRM prediction. Blue line indicates the CMG prediction.

Chapter 6 Conclusions and Future Work

6.1 Conclusions

The objective of this research is to characterize a tight oil reservoir and gain a better understanding of its heterogeneity. After extensive literature reviews on several tools that can be used to achieve this goal, the CRM model is selected. Since the CRM model requires only injection data and production data as input, it becomes very practical to evaluate a reservoir. The CRM model is applied to a tight oil reservoir through inputting field injection and production data. The nonlinear multivariate optimization technique required to determine parameters in the CRM model is achieved by coding in MATLAB. Through analyzing the results of the CRM model, the following conclusions can be drawn:

1. In a heterogeneous tight oil reservoir, the assumption that the injectors are only connected with surrounding producers is very useful for the CRM model application. This will significantly reduce the number of unknown parameters.
2. Some producers that benefit from the injection are identified. If the connectivity between an injector/producer pair is high and the time constant is small, one can conclude that the producer benefits from that particular injection well.
3. Most injected water remains around the injectors and then pressurized regional areas surrounding the injectors. For many injector/producer pairs, the presence of large time constant with high connectivity indicates most

injected water is stored in the interwell regions and the pressure of the interwell regions will increase consequently.

4. The production rates are predicted to December of 2019 by the CRM model and CMG full field model. The results are shown and discussed to conclude that the CRM model provides a more reasonable prediction result.

6.2 Recommended Future Works

The algorithm and techniques associated with this particular nonlinear optimization problem can be investigated more deeply. Moreover, the relationship between the results and the parameter constraints as well as initial guess of this large scale optimization problem needs to be investigated.

References

Albertoni, A., & Lake, L.W. 2003. Inferring Connectivity Only From Well-Rate Fluctuations in Waterfloods. *SPE Res Eval. & Eng.* **6:** 6-16. SPE-83381-PA. http://dx.doi.org/10.2118/83381-PA.

Anna, L.O. 2009. Geologic Assessment of Undiscovered Oil and Gas in the Powder River Basin Province, Wyoming and Montana. U.S. Deparment of the Interior and U.S. Geological Survey.

Araujo, H., Gilman, J.R., & Kazemi, H. 1998. Analysis of Interference and Pulse Tests in Heterogeneous Naturally Fractured Reservoirs. Paper SPE 49234, presented at the 1998 SPE Annual Technical Conference and Exhibition, New Orleans, LA, 27-30 September. http://doi.org/10.2118/49234-MS.

Cao, F. 2014. Development of A Two-Phase Flow Coupled Capacitance Resistance Model. Ph.D. Dissertation. The University of Texas at Austin, Austin, Texas.

Cockin, A.P., Malcolm, L.T., McGuire, P.L., Giordano, R.M., & Sitz, C.D. 2000. Analysis of A Single-Well Chemical Tracer Test to Measure the Residual Oil Saturation to A Hydrocarbon Miscible Gas Flood at Prudhoe Bay. *SPE Res Eval. & Eng.* **3:** 544-551. SPE-68051-PA. https://doi.org/10.2118/68051-PA.

Dhooge, J.A., Sheely, C.Q., & Williams, B.J. 1981. Interwell Tracers - An Effective Reservoir Evaluation Tool: West Sumatra Field Results. *J. Pet Tech* **33** (05): 779-782. SPE-8434-PA. http://doi.org/10.2118/8434-PA.

Dolton, G.L., Fox, F.E., & Clayton, J.L. 1990. Petroleum Geology of the Powder River Basin, Wyoming and Montana. U.S. Geological Survey Open-File Report.

Du, Y., & Guan, L. 2005. Interwell Tracer Tests: Lessons Learned from Past Field Studies. Paper SPE 93140, presented at the SPE Asia Pacific Oil and Gas Conference and Exhibition, Jakarta, 5-7 April. http://dx.doi.org/10.2118/93140-MS.

Gentil, P.H. 2005. The Use of Multilinear Regression Models in Patterned Waterfloods: Physical Meaning of the Regression Coefficients, M.S. Thesis, The University of Texas at Austin, Austin, Texas.

Ingle, T., Ketter, C., Anderson, D.M., & Thompson, J.M. 2017. Practical Completion Design Optimization in the Poweder River Basin - An Operator Case Study. Paper SPE 185064, presented at the SPE Unconventional Resource Conference, Calgary, Alberta, Canada, 15-16 February. http://doi.org/10.2118/185064-MS.

Kaufman, R.L., Dashti, H., Kabir, C.S., Pederson, J.M., Moon, M.S., Quttainah, R., & Al-Wael, H. 1997. Characterizing The Greater Burgan Field: Use of Gepchemistry and Oil fingerprinting. Paper SPE 37803, presented at the 10th SPE Middle East Oil Show and Conference, Bahrain, 15-18 March. http://doi.org/10.2118/37803-MS.

Kamal, M.M. 1983. Interference and Pulse Testing-A Review. *J Pet Tech* **35** (12): 2257-2270. SPE-10042-PA. http://doi.org/10.2118/10042-PA.

Kaviani, D., Jensen, J.L., & Lake, L.W. 2012. Estimation of Interwell Connectivity in the Case of Unmeasured Fluctuating Bottomhole Pressure. *J. Pet. Sci. Eng.* **90-91:** 79-95. http://dx.doi.org/10.1016/j.petrol.2012.04.008.

Larter, L.R., & Aplin, A.C. 1994. Production Applications of Reservoir Geochemistry: A Current and Long-Term View. Paper SPE 28375, presented at the SPE 69th Annual Technical Conference and Exhibition, New Orleans, 25-28 September. http://doi.org/10.2118/28375-MS.

Liang, X., Weber, D.B., Edgar, T.F., Lake, L.W., Sayarpour, M. & Yousef, A.A. 2007. Optimization of Oil Production Based on a Capacitance Model of Production and Injection Rates. Paper SPE 107713, presented at the 2007 SPE Hydrocarbon Economics and Evaluation Symposium, Dalls, TX, 1-3 April. http://doi.org/10.2118/107713-MS.

Ruhle, W., & Orth, J. 2015. Production Trends from the Exploitation of Horizontal Completions in the Upper Cretaceous Formations of the Powder River Basin: A Look Back on Five Years of Development. Paper SPE 175957, presented at the SPE/CSUR Unconventional Resources Conference, Calgary, Alberta, Canada, 20-22 October. http://doi.org/10.2118/175957-MS.

Sayarpour, M., Zuluaga, E., Kabir, C.S., & Lake, L.W. 2009. The Use of Capacitance-Resistance Models for Rapid Estimation of Water-flood Performance and Optimization. *J. Pet. Sci. Eng.* doi: 10.1016/j.petrol.2009.09.006.

Sinha, R., Asakawa, K., & Pope, G.A. 2004. Simulation of Natural and Partitioning Interwell Tracers to Calculate Saturation and Swept Volumes in Oil Reservoirs. Paper SPE 89458, presented at the 2004 SPE/DOE Fourteenth Symposium on Improved Oil Recovery, Tulsa, Oklahoma, 17-21 April.

Slentz, L.W. 1981. Geochemistry of Reservoir Fluids as Unique Approach to Optimum Reservoir Management. Paper SPE 9582, presented at the SPE Middle East Oil Technical Conference, Bahrain, 9-12 March. https://doi.org/10.2118/9582-MS.

Soroush, M., Jensen, J., & Kaviani, D. 2013. Interwell Connectivity Evaluation in Cases of Frequent Production Interruptions. Paper SPE 165567, presented at the 2013 SPE Heavy Oil Conference, Calgary, Alberta, Canada, 11-13 June.

Tian, W. 2017. Improved Method of Moments to Determine Mobile Phase Saturations with Single Well Chemical Tracer Test. Paper SPE 189300, presented at the SPE Annual Technical Conference and Exhibition, San Antonio, Texas, 9-11 October. http://doi.org/10.2118/189300-STU.

Vela, S., & McKinley, R.M. 1970. How Areal Heterogeneities Affect Pulse - Test Results. *J Pet Tech* **10** (2). http://doi.org/10.2118/2569-PA.

Wagner, O.R. 1977. The Use of Tracers in Diagnosing Interwell Reservoir Heterogeneities - Field Results. *J Pet Tech* **29** (11): 1410-1416. SPE-6046-PA. https://doi.org/10.2118/6046-PA.

Walsh, M.P., & Lake, L.W. 2003. *A Gneralized Approach to Primary Hydrocarbon Recovery*. Amsterdam: Elsevier Science.

Wilson, M.D. 1982. Origins of Clays Controlling Permeability in Tight Gas Sands. *J Pet Tech* **34** (12): 2871-2876. http://doi.org/10.2118/9843-PA.

Woods, E.G. 1970. Pulse-Test Response of a Two-Zone Reservoir. *SPE J.* **10** (3): 245-256. SPE-2570-PA. http://dx.doi.org/10.2118/2570-PA.

Yousef, A.A., Gentil, P.H., Jensen, J.L., & Lake, L.W. 2006. A Capacitance Model to Infer Interwell Connectivity From Production and Injection Rate Fluctuations. *SPE Res Eval & Eng* **9** (6): 630-646. SPE-95322-PA. http://dx.doi.org/10.2118/95322-PA.

Yousef, A.A., Gentil, P.H., Jensen, J.L., & Lake, L.W. 2005. A Capacitance Model to Infer Interwell Connectivity From Production and Injection Rate Fluctuations. Paper SPE 95322, presented at the SPE Annual Technical Conference and Exhibition, Dallas, TX, 9-12 October. http://doi.org/10.2118/95322-MS.

Appendix A: Nomenclature

Symbols

c_o	Oil compressibility (L^2/F)
c_w	Water compressibility (L^2/F)
c_t	Total reservoir compressibility (L^2/F)
β_{ij}	Interwell connectivity between injector *i* and producer *j*
τ_{ij}	Time constant between injector *i* and producer *j*, (t)
J	Productivity index (L^5/Ft)
N_{inj}	Total number of injection wells
N_{pro}	Total number of production wells
p_{wf}	Bottom hole flowing pressure (F/L^2)
p'_{wf}	Effective bottom hole flowing pressure (F/L^2)
$\bar{p}$	Average reservoir pressure (F/L^2)
S	Saturation
S_O	Oil saturation
S_w	Water saturation
t	Time (t)
q	Fluid production rates (L^3/t)
T	Transmissibility (L^5/Ft)
$\hat{q}_j$	Modeled liquid production rates (L^3/t)
n	Time-like variable
ν_{kj}	Coefficients of the bottom hole pressure term in the CRM model
i'_{ij}	Effective injection rates (L^3/t)
i_{ij}	Actual injection rates (L^3/t)

Subscripts and superscripts

i	Injector index
j	Producer index
k	Producer bottom hole pressure index

Appendix B: MATLAB Code

```
clear all
l;

MaxIter=200;
nspsa=10;
lambda0=0.001;
A=20;
alpha=0.602;
gamma=0.101;
c0=0.0000001;
gradtype=1;

%input

primarypro=load('primary.txt')

pro=load('pro.dat');
[Nt1 Npro]=size(pro);
inj=load('inj.dat');
[Nt2 Ninj]=size(inj);
Nt=min(Nt1,Nt2);

 %sun all input
T_index=Nt;
Num_uncond=1;
Ndobs=T_index*Npro;


dobs_index=[];
dobs=[];
 for i=1:T_index
    dobs=[dobs pro(i,:)];
    if min(abs(pro(i,:)))==0.0
       dobs_index=[dobs_index zeros(1,Npro)];
    else
       dobs_index=[dobs_index ones(1,Npro)];
    end
  end
covd=(dobs*0.05+5).^2;
%covd(1:Ndobs)=1.0;

%initial guess

lamd=ones(Npro,Ninj)*(1/Npro);
```

```
tao=ones(Npro,Ninj)*10;
% tao=0.25./lamd;
blp=zeros(Npro,1);
dim_m=(Ninj*2+1)*Npro;


m_pr=[];
 m_up=[];
 m_low=[];
covm=[];

%input constrain information

for i=1:Npro
    m_pr=[m_pr lamd(i,:)];
    m_pr=[m_pr tao(i,:)];
    m_pr=[m_pr blp(i,1)];

    covm=[covm ones(1,Ninj)*0.25];
    covm=[covm ones(1,Ninj)*1.0];
    covm=[covm 1.0];
    m_up=[m_up ones(1,Ninj)*1.0 ones(1,Ninj)*1.0E4 1000];
   m_low=[m_low ones(1,Ninj)*0.000000001  ones(1,Ninj)*0.0000000001  -0.001];
end

Aeq=zeros(Ninj,dim_m);
Beq=ones(Ninj,1);

for i=1:Ninj
    for j=1:Npro
        indx=(j-1)*(Ninj*2+1)+i;
        Aeq(i,indx)=1;
    end
end


 MAP=[];
 Obj_iter=zeros(MaxIter+1,Num_uncond);


 for m_index=1:Num_uncond
    if Num_uncond==1
     m_uc(:,m_index)=m_pr';
     d_uc(:,m_index)=dobs';
    end
   m0=m_uc(:,m_index);
```

```
muc_g(:,m_index)=get_dobs(m0,inj,T_index,d_uc(:,m_index),dobs_index,Npro,Ninj,primarypro);

obj=get_obj(m0,m_uc(:,m_index),d_uc(:,m_index),inj,T_index,dobs_index,Npro,Ninj,covm,covd,primarypro);
   Obj_iter(1,m_index)=obj;

   %nonlinear optimization

   OPTIONS=optimset('Display','iter','GradObj' ,'off','Algorithm','interior-point','TolFun',1e-9,'MaxIter',200);

[m,FVAL]=fmincon(@(m)get_obj(m,m_uc(:,m_index),d_uc(:,m_index),inj,T_index,dobs_index,Npro,Ninj,covm,covd,primarypro),m0,[],[],Aeq,Beq,m_low,m_up,[], OPTIONS);
%[m,FVAL]=FMINCON(@(m)get_obj(m,m_uc(:,m_index),d_uc(:,m_index),inj,T_index,Npro,Ninj,covm,covd),m0,[],[],[],[],m_low',m_up',[], OPTIONS);
   B=Aeq*m;
  MAP=[MAP m];
muc_g1(:,m_index)=get_dobs(m,inj,T_index,d_uc(:,m_index),dobs_index,Npro,Ninj,primarypro);

 end

 %output fitting result

 m_map=mean(MAP,2);
 mapdobs=get_dobs(m_map,inj,T_index,dobs',dobs_index,Npro,Ninj,primarypro);

 %output result

 for j=1:Npro
    lamda(j,:)=m_map(((j-1)*(Ninj*2+1)+1):(j*(Ninj*2+1)));
 end



  map_pro=zeros(T_index,Npro);
  mucg_pro=zeros(T_index,Npro);
   for i=1:T_index
     map_pro(i,:)=mapdobs((i-1)*Npro+1:i*Npro);
     mucg_pro(i,:)=muc_g((i-1)*Npro+1:i*Npro,1);
   end
```

```
for i=1:Npro
    figure;
   plot(map_pro(1:T_index,i),'b','LineWidth',2.0);
   hold on;
   plot(pro(1:T_index,i),'ro','MarkerFaceColor','r');
   xlabel('Time (months)');
   ylabel('Rates B/D');
   legend('CRM Model','Actual Data','location','northeast');
  saveas2(['well' num2str(i,'%4.4i') '.pdf'],'300');
end

%calculated production rates based on known parameters

function gm=get_dobs(m,inj,Nt,dobs,dobs_index,Npro,Ninj,primary)
gm=[];
pro=zeros(Nt,Npro);

for j=1:Npro
      lamd=[];
    lamd=m(((j-1)*(Ninj*2+1)+1):((j-1)*(Ninj*2+1)+Ninj));
    tao=m(((j-1)*(2*Ninj+1)+Ninj+1):((j-1)*(2*Ninj+1)+2*Ninj))+0.1e-13;

    for n=1:Nt

        for i=1:Ninj
            injbar(n,i)=0.0;

            for mm=1:n
                index=(j-1)*(Ninj+2)+Ninj+1;
                injbar(n,i)=injbar(n,i)+inj(mm,i)*exp((mm-n)/tao(i,1))*(1-exp(-1/tao(i,1)));
            end

        end
       pro(n,j)=lamd'*injbar(n,:)'+m(j*(Ninj*2+1))+primary(j)*exp(-n/tao(1,1));

        if dobs_index((n-1)*Npro+j)==0
          pro(n,j)=dobs((n-1)*Npro+j);
         end
    end

end
 for i=1:Nt
    gm=[gm pro(i,:)];
 end
end
```

```
%calculate objective funciton (the difference between calculated production
%rates real produciton rates)

function
[Om]=get_obj(m,m_uc,d_uc,inj,T_index,dobs_index,Npro,Ninj,covm,covd,primary)

gm=get_dobs(m,inj,T_index,d_uc,dobs_index,Npro,Ninj,primary);


t=length(d_uc);

 tempd=(d_uc'-gm);
 gmd=0.5*(tempd./covd)*tempd';
 gmm=0.5*((m-m_uc)'./covm)*(m-m_uc);

 Om=gmd;


end
```